In vitro expansion of bone marrow multipotent mesenchymal stromal cells: Effects of different incubator gas tensions

Tommy Aleksander Karlsen

Master thesis

Department of Molecular Biosciences

UNIVERSITY OF OSLO

August 2007

Acknowledgements

The work in this thesis was performed at the Institute of Immunology, Faculty Division Rikshospitalet, University of Oslo.

I would like to thank:

My supervisor, Dr. Jan E. Brinchmann, for his advices during this master thesis, and for always being helpful and answering my questions.

My internal supervisor, Professor Tor Lea, for valuable feedback during the writing process.

Aboulghassem Shahdadfar for teaching me all the cell culture procedures, and for his many helpful talks and advices.

Shivali Duggal for her valuable help during the microarray analysis.

The whole cell therapy group for an including and inspiring working environment.

Tuva Barøy and Trude Movig for proofreading my thesis.

Glenn Karlsen for help to create figure 1-1, 2-2, 2-4 and 2-5.

My family and friends for support.

Abstract

Human bone marrow multipotent mesenchymal stromal cells (hBM-MSC) represent an appealing source of adult stem cells for cell therapy and tissue engineering. Since hBM-MSC are present at low frequency in the bone marrow, *in vitro* expansion is necessary prior to performing clinical studies. Standard incubator gas tensions corresponding to 20% O_2 and 5% CO_2 are routinely used for *in vitro* expansion of hBM-MSC, and it is being overlooked that such conditions do not correspond to the physiological gas tensions found in the bone marrow microenvironment. To explore the effects of different gas tensions, polyclonal hBM-MSC from three donors were expanded in 6 different combinations of O_2 and CO_2 tensions. Phase contrast microscopy was used to determine cell morphological features, growth curves were made to assess differences in proliferative capability, real-time RT PCR was used to measure gene expression of markers associated with undifferentiated embryonic stem cells, and microarray analysis was performed to assess the global gene expression of the cells. No change in morphology could be observed between hBM-MSC cultured in the different gas tensions. The results from the growth curves indicated that gas tensions did not affect the proliferative capability of the cells. Real-time RT PCR data showed no consistent difference in gene expression between the culture conditions. According to the microarray analysis, there was no significant difference in global gene expression between hBM-MSC cultured in the different gas tensions.

Most current protocols for *in vitro* culture of hBM-MSC include fetal bovine serum (FBS) as nutritional supplement. When culturing hBM-MSC in FBS, depletion of $CD14^+$ monocytes seems to be necessary in order to avoid monocyte contamination in the cultures. In this study, FBS was replaced by autologous serum (AS). As a part of this thesis, the necessity of depleting $CD14^+$ cells when expanding hBM-MSC in AS was investigated. Only minor contamination of monocytes was observed in the non-depleted cultures, indicating that there is no need to deplete $CD14^+$ cells when expanding hBM-MSC in AS.

Table of contents

Abbreviations

alloHS	Allogeneic human serum
AS	Autologous serum
ASC	Adult stem cells
BM-MNC	Bone marrow-mononuclear cells
BMP	Bone morphogenetic protein
CFU-F	Colony forming unit-fibroblasts
DMSO	Dimethyl sulfoxide
ECC	Embryonic carcinoma cells
ESC	Embryonic stem cells
FBS	Fetal bovine serum
GAPDH	Glyceraldehyde-3-phosphate dehydrogenase
GDF	Growth and differentiation factor
GvHD	Graft-versus-host disease
hAT-MSC	Human adipose-derived multipotent mesenchymal stromal cells
hBM-MSC	Human bone marrow multipotent mesenchymal stromal cells
HSC	Hematopoietic stem cells
ICM	Inner cell mass
ISCT	International Society for Cellular Therapy
MAPC	Multipotent adult progenitor cells
mAT-MSC	Murine adipose multipotent mesenchymal stromal cells
MSC	Multipotent mesenchymal stromal cells
Nf-κB	Nuclear factor-kappa B
NSC	Neural stem cell
OD	Optical density
PCR	Polymerase chain reaction
PGC	Primordial germ cells
PPAR-γ	Receptor peroxisome proliferator-activated receptor-γ
RIN	RNA integrity number
rBM-MSC	Rat bone marrow multipotent mesenchymal stromal cells
ROS	Reactive oxygen species
RQ	Relative quantification
RT	Reverse transcription
SESC	Skin epithelial stem cells
TAE	Tris-acetate-EDTA
TGF-β	Transforming growth factor-β
TNFα	Tumor necrosis factor α
Wnt	Wingless-type MMTV integration site family

1. Introduction

1.1 Stem cells

Over the past few years, stem cell research has received tremendous interest from scientists, because of its suggested potential to provide cures or new treatment modalities for numerous incurable diseases and injuries. Many questions about stem cells remain unanswered since the field of stem cell research is still in its early stages. Clearly, further research will provide some of these answers, but like any scientific field, stem cell research raises as many questions as it answers.

A stem cell, by definition, is an undifferentiated (unspecialized) cell that can produce both new stem cells (self-renewal), and cells that commit to a pathway leading to differentiation[1] (Figure 1-1).

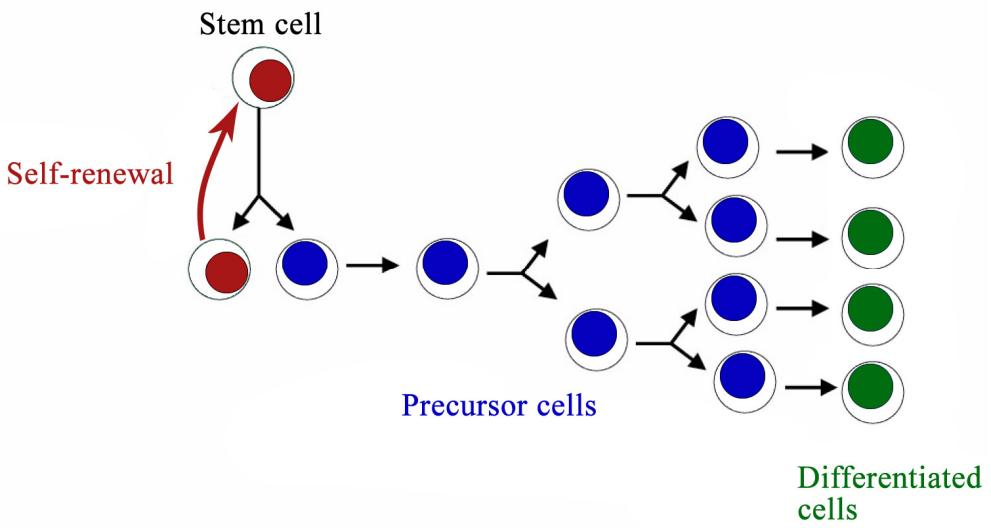

Figure 1-1. A stem cell is an undifferentiated cell that has the ability to reproduce itself in a process called self-renewal. It also can differentiate and give rise to specialized cells that make up tissues and organs of the body. In adult and fetal tissues, the daughter cells committed to differentiation first become precursor cells. These can divide symmetrically to form more precursor cells, or differentiate further to become organ specific, end-differentiated cells.

Differentiation is a process where an unspecialized cell changes to acquire features typical of cells of one of the organs in the body. Stem cells remain uncommitted and in a slowly proliferating state *in vivo*, until they receive a signal to develop into a specialized cell[2]. This differentiation signal triggers altered expression of genes involved in cell division and differentiation. Depending on the signal provided, the cells can undergo both symmetric

division (identical daughter cells) and asymmetric division (non-identical daughter cells) in order to maintain or expand the stem cell pool and to produce differentiated progeny. Some stem cells can produce a variety of differentiated cells[3], while other stem cells only generate a few, or one type differentiated cells. Stem cells in the testis, for example, produce only one type differentiated cells (the spermatozoa)[4].

1.2 Classification of stem cells

1.2.1 Embryonic stem cells

Animals start their life as a fertilized egg referred to as a zygote (figure 1-2). The zygote is totipotent[5], meaning that it is capable of giving rise to all the cell types found in animals, including those that do not form part of the embryo, such as the cells of the placenta and umbilical cord. A complex cascade of gene regulation drives the zygote through several rounds of mitotic division called cleavage, resulting in gradually smaller cells. Between four and six days after fertilization the cells are arranged into two regions, an outer layer called the trophectoderm (or trophoblast) which is involved in implantation and formation of the placenta, and an inner core of cells called the inner cell mass (ICM). At this stage the embryo is referred to as a blastocyst[6, 7]. During development the ICM develops into two distinct cell layers, the epiblast and hypoblast. The hypoblast gives rise to the yolk sac, and the epiblast gives rise to the three primary germ layers (ectoderm, endoderm, and mesoderm). The three germ layers further develop into all the cells and organs that make up the adult body (figure 1-2). Another type of cells called primordial germ cells (PGC), which reside in a specific part of the embryo called the gonadal ridge, give rise to the germ cells (eggs and sperm).

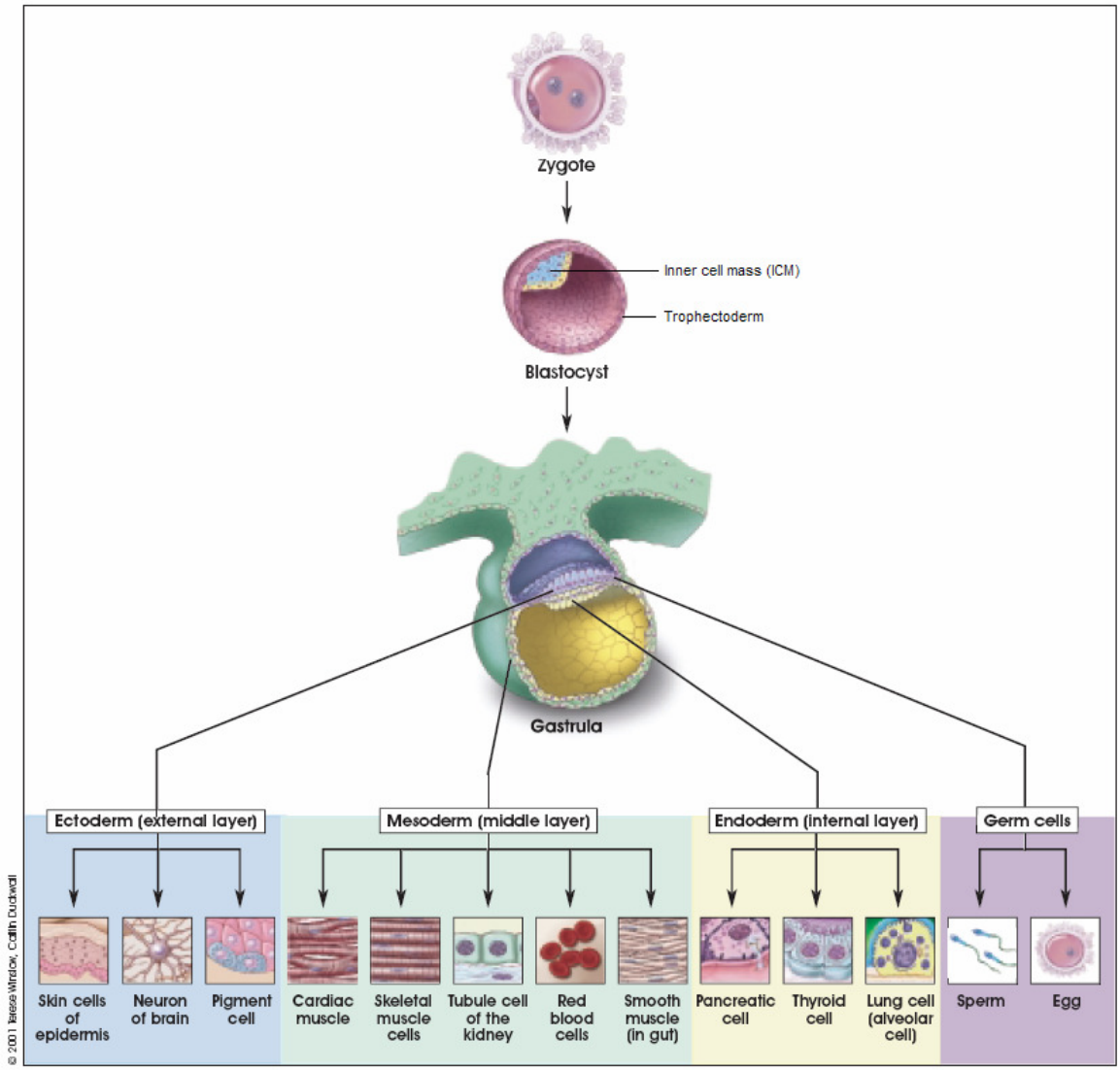

Figure 1-2. Major types of cells differentiated from the germ layer cells (Reprinted from Stem cells: Scientific progress and future research directions – a stem cell report from The National Institutes of Health june 17, 2001, with permission from Terese Winslow).

Embryonic stem cells (ESC) are derived by removing the ICM from the blastocyst, and growing the cells *in vitro* in a laboratory culture dish (figure 1-3). These cells are undifferentiated, they can proliferate indefinitely in culture, and they are capable of giving rise to all the cells in the adult body[3, 8]. Cells with this capability are said to be pluripotent. The difference between the totipotent zygote and the pluripotent ESC, is that the ESC can only generate cells that form part of the embryo, and lack the ability of the zygote to form extraembryonic tissues[8].

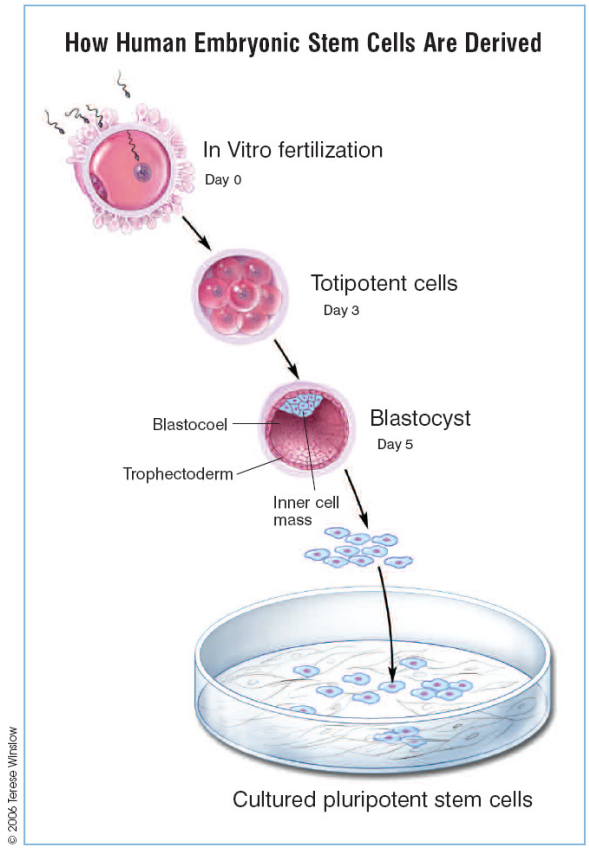

Figure 1-3. Derivation of human ESC. Approximately five days after *in vitro* fertilization a blastocyst develops. ESC (pluripotent stem cells) are derived by removing the ICM from the blastocyst, and culturing the cells *in vitro*. (Reprinted from Regenerative medicine 2006 - a stem cell report from The National Institutes of Health, with permission from Terese Winslow).

Several proteins play a central role in directing self-renewal and maintaining pluripotency of ESC. Among these are the transcription factors Oct-4[9], Nanog[10], Sox2[11], c-Myc [12] and Klf-4[10]. Recently, Takahashi *et al.* demonstrated that pluripotency in mouse embryonic and adult fibroblasts was induced by introducing Oct-4, Sox2, c-Myc and Klf-4, under ESC culture conditions[13]. These transcription factors activate transcription of genes that are essential for pluripotency and suppress genes that are responsible for differentiation. The regulation of these transcription factors and the mechanism by which they work to maintain pluripotency are not fully understood.

1.2.2 Adult stem cells

Most, if not all, adult organs in the body contain stem cells, which are referred to as adult stem cells (ASC). These cells have a more restricted differentiation potential compared to the ESC, and lack the capability of the ESC of unlimited proliferation in culture. Stem cells with limited differentiation potential are often called multipotent stem cells. Originally, it was thought that ASC could only differentiate into the cell types of the organ/tissue from which

they originated. However, more recent studies have described differentiation of ASC into mature phenotypes that are different from their organ/tissue of origin[14, 15], leaving this topic controversial[16].

Throughout life, billions of dead cells are replaced by new cells every day in order to maintain tissue homeostasis. The main function of the ASC is to regenerate and repair the tissues in which they reside. Normally, ASC produce progenitor cells, which proliferate before they differentiate into the mature cells that are being replaced (figure 1-1). ASC are different in part because, in the tissues, they have their own specialized environment called niche[2, 17]. For most stem cells the niche is poorly defined, but it is a complex microenvironment composed of extracellular matrix, differentiated cells, stem cells and their progeny, and factors secreted by the cells. The fate of the stem cells is controlled by this niche[2]. Very few ASC exist in each tissue, thereby making it a challenge to isolate them in the laboratory. Cells contain proteins called antigens, or surface markers, in their cell membranes. Each cell type has a different set of surface markers, protruding from the cell's surface. By taking advantage of the uniqueness of these markers, different cells can be isolated and identified by modern techniques of cell biology.

1.3 Why study stem cells?

As a result of their ability to self-renew and their differentiation potential, stem cells are believed to have the potential to cure or treat a number of chronic diseases and injuries, such as diabetes, multiple sclerosis, heart diseases, Parkinson's disease, osteoporosis, and spinal injuries[18].

Stem cells could potentially provide cells and tissues for transplantation therapy. Some diseases and injuries are caused by the death or dysfunction of one or a few cell types, for example diabetes, Parkinson's disease, and spinal injuries. If such cells can be replaced by new functional cells made from stem cells, it could offer a lifelong treatment for these diseases or injuries. Furthermore, stem cells could potentially offer human tissues and cells that can be used for testing new human drugs. Often animal models are being used for these experiments, but drugs do not always have the same effect on humans as on animals because of species-specific differences. By having pure populations of human cells that are affected by a disease, new drugs could be tested in cultures of these cells. The same populations of cells

may also be used for toxicity testing. Populations of stem cells are also predicted to have a future application for preventing the development of a disease. For example, a supply of neuronal cells could be studied in detail to understand the mechanism of cell death in Parkinson's disease.

Following introduction of genes into stem cells by genetic engineering, the cells could be introduced into the body in order to produces proteins that act as therapeutic agents. This approach is called gene therapy.

Due to lack of organ donors and limitations because of immunological rejections and physical size, stem cells may provide ways for obtaining tissues and organs for transplantation (tissue engineering). The patient's own cells could be seeded on a bio-degradable scaffold that could allow the formation of a particular tissue.

Studying cell differentiation will be important for the understanding of fundamental events in embryonic development that one day may explain the causes of birth defects and how to prevent them. It will also give valuable information that may help in understanding the development and function of cells and organs.

In the future, stem cell research could conceivably give new technology and treatment options that scientists currently are unaware of.

1.4 Adult stem cells versus embryonic stem cells

Source and differentiation- and proliferation potential are probably the most important differences between ESC and ASC. Because ESC are derived from fertilized eggs that are destroyed during the procedure, there are ethical considerations concerning the use of these cells. Use of ASC is not associated with these same ethical issues because they are derived from borne individuals, so their derivation does not involve the destruction of a blastocyst, and also an informed consent can be given. It has therefore been argued that use of ESC should be avoided and the focus should be on ASC only. Today, most scientists agree that investigation of both types of cells is necessary to understand how these cells can be used in therapy. The advantages of ESC are that they can be expanded for many generations in an undifferentiated state and they can differentiate into all cell types in the body. Thus, in theory,

all cell types can be produced in quantities required for clinical applications. However, in spite of their promising potential, the use of ESC are not ready to be applied in therapy. The mechanisms behind differentiation are poorly understood, and the cells often differentiate spontaneously. When transplanted into a host, ESC frequently develop into teratomas (tumors). Pre-differentiation of ESC has been shown to decrease the likelihood of teratoma formation, and could represent a possible solution to this clinical obstacle. Human ESC-derived oligodendrocyte progenitors did not show any signs of teratoma development after being transplanted into rats[19]. It is not known why pre-differentiated ESC do not develop into teratomas, but they could possibly have developed to a stage where they are restricted to differentiate into only one specific lineage. As they have differentiated beyond the point where differentiation to many different lineages is possible, they are not able to produce teratomas. Another limitation for the use of ESC is rejection of the cells after transplantation. ESC contain the donor's HLA molecules in the cell membrane, and if the donor and recipient do not have the same set of HLA molecules when cells/tissues are transplanted from one person to another, the transplanted cells will be rejected by the recipient's immune system[20]. Therefore, the recipient must use immunosuppressive drugs, which frequently cause severe side effects, to prevent rejection of the cells.

Even though ASC have a more restricted differentiation and dividing potential compared to the ESC, they nevertheless have potential for treating diseases. Bone marrow transplantation, or hematopoietic stem cell transplantation, has been used in the clinic for decades, and several other clinical trials with ASC have shown promising results[21, 22]. Cancer development (teratomas) has not been observed for ASC used in humans. It has been suggested that stem cells that are injected into the body tend to migrate towards the site of injury, and that the surroundings of the injury can induce differentiation into the cell types required to repair the damaged cells/tissues[23]. Ideally, the patients own cells will be used in order to avoid rejection by the recipient, thereby avoiding the need for immunosuppressive drugs.

1.5 Multipotent mesenchymal stromal cells

1.5.1 Sources of multipotent mesenchymal stromal cells

Multipotent mesenchymal stromal cells (MSC), previously referred to as mesenchymal stem cells, are multipotent, non-hematopoietic stem cells that are usually isolated from bone

marrow[24-27] or adipose tissue[28, 29], but can also be isolated from several other tissues such as skeletal muscle[30], trabecular bone[31], dermis[32], blood[33], periosteum[34], teeth[35], synovial membrane[36], amniotic fluid[37], placenta[38] and umbilical cord blood[39].

1.5.2 Properties of human MSC

MSC were first described by Friedenstein *et al.* more than three decades ago as colony forming unit-fibroblasts (CFU-F) because of their ability to adhere to plastic surfaces and form fibroblast-like colonies when plated at low densities[25]. This process involves flattening and spreading of the cells into their characteristic spindle-shape, which is very similar to that of fibroblasts (figure 1-4). In the microscope, MSC cultures appear to be a rather homogenous population of fibroblast-like cells. In fact, they consist of a heterogeneous group of progenitor cells with varying proliferation and differentiation potentials[40, 41].

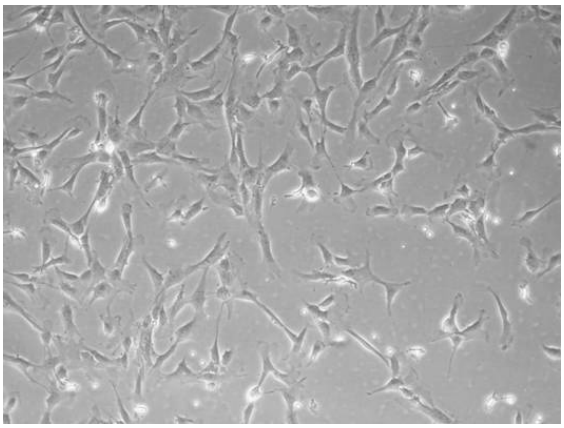

Figure 1-4. Human MSC in culture.
In vitro MSC have a shape resembling fibroblasts. Image magnified 200 X.

Laboratories around the world use relatively different isolation and expansion methods, and also different approaches to characterize MSC. This makes it difficult to compare results between laboratories since it is not known if the cell populations are similar enough for direct comparison. Therefore, the Mesenchymal and Tissue Stem Cell Committee of the International Society for Cellular Therapy (ISCT) has proposed three criteria to define human MSC [42]. First, the cells must adhere to plastic surfaces when cultured in tissue culture flasks. This is a well described property of MSC and is utilized for isolating the cells. Second, MSC should have a specific surface marker profile, and 95%, or more, of the MSC population should express CD105 (also known as endoglin), CD73 (also known as ecto 5' nucleotidase), and CD90 (also known as Thy-1). MSC populations can often be contaminated with other

cells, especially hematopoietic cells. To ensure that the MSC populations are pure it is recommended that cultured MSC lack expression (≤ 2 % positive) of the hematopoietic stem cell marker CD34, the hematopoietic cell marker CD45, one of the two macrophage markers CD14 and CD11b and one of the two B-cell markers CD79α and CD19. HLA DR, which is expressed on professional antigen-presenting cells such as dendritic cells, B-cells and macrophages, should also be negative, but this molecule can be expressed by MSC if they are stimulated with interferon-γ[43]. If this is the case another term, for example "stimulated MSC", should be used to distinguish them from the unstimulated MSC. Third, the cells must be able to differentiate to osteocytes, chondrocytes and adipocytes *in vitro*. These criteria are minimal requirements and apply only to human MSC. MSC from other species also display plastic-adherence and trilineage differentiation, but the surface marker expression can vary between species[44]. As the field of MSC makes progress, these criteria will most likely require modifications, but with the current state of knowledge this is the best way of defining human MSC. By employing these criteria in studies the comparison between laboratories will most likely be facilitated and advance the progression in the MSC field.

1.5.3 Human bone marrow multipotent mesenchymal stromal cells

Human marrow multipotent mesenchymal stromal cells (hBM-MSC) are found at a very low frequency in the bone marrow. It has been estimated that hBM-MSC constitute between 0.001% and 0.01% of the total population of nucleated cells in the bone marrow [24, 26]. Due to this low frequency of hBM-MSC in the bone marrow, *in vitro* expansion of the cells is necessary prior to clinical studies. Both *in vitro* and *in vivo*, studies have shown that hBM-MSC can differentiate into cells of mesodermal origin including osteocytes, chondrocytes and adipocytes[26, 45], as well as tenocytes[46], cardiomyocytes[47, 48] and skeletal muscle[49] (figure 1-5). There is evidence that hBM-MSC also possess the ability of differentiating into cells of non-mesodermal lineages such as neural precursors[49, 50] and hepatocyte-like cells[51].

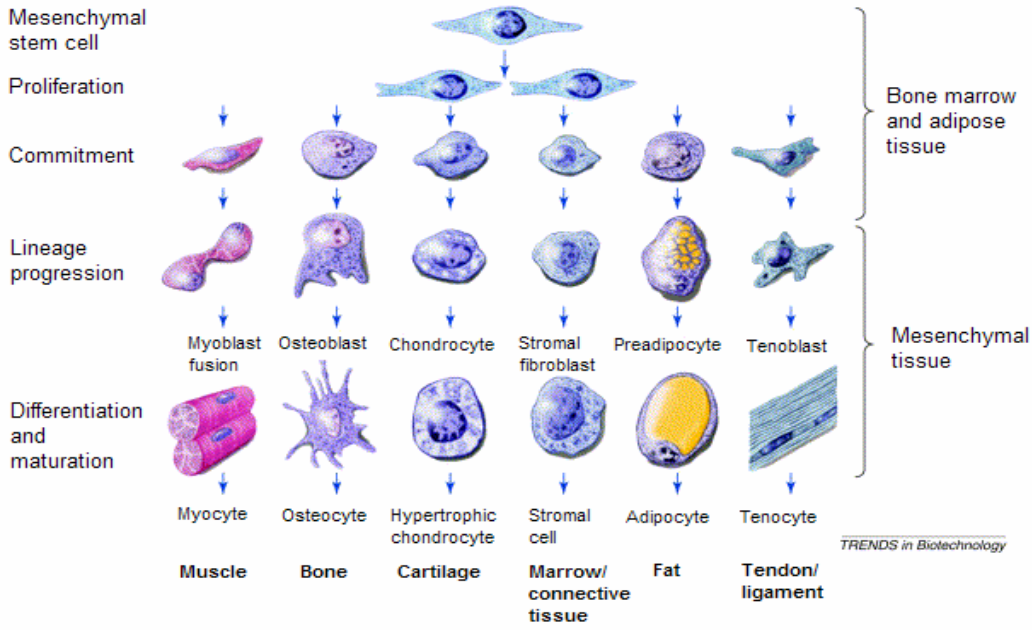

Figure 1-5. MSC can give rise to several mesodermal cell types indicated in the figure. See text for details. (Reprinted from Trends in biotechnology, volume 20, No 8, Makarand D. Risbud and Michael Sittinger, Tissue engineering: advances in *in vitro* cartilage generation, page 351-356, August 2002, with permission from Elsevier)

Because of their ease of isolation and extensive differentiation potential, as well as their high *in vitro* expansion potential, hBM-MSC have been well characterized, and they are believed to have a great potential for cell therapy and tissue engineering. The hBM-MSC have demonstrated efficacy in clinical trials in children with osteogenesis imperfecta[21, 22] and it has furthermore been shown that hBM-MSC might enhance engraftment and treat graft-versus-host disease (GvHD) in allogeneic stem cell transplantation[52-55]. However, most information about hBM-MSC biology (MSC in general) has been derived from *in vitro* studies. Thus, little is known about the biology of these cells *in vivo*.

1.5.4 hBM-MSC cell surface molecules

As described above, ISCT has proposed minimum criteria for surface marker expression in human MSC. However, most laboratories test for other surface markers as well, both positive and negative, to get additional evidence. Because hBM-MSC populations are heterogeneous within the cultures, variable expression of markers can be observed. Today, autologous serum (AS) and foetal bovine serum (FBS) is commonly used when expanding hBM-MSC *in vitro*. There is a small difference in cell surface molecule expression when comparing hBM-MSC cultured in medium containing AS compared to that of FBS[24] (table 1-1). None of the surface markers included in table 1-1, or in the minimum criteria from the ISCT, are cell-specific for

hBM-MSC, they are all expressed on other cells as well. Taken together, this illustrates the challenge of identifying these cells solely by surface markers, and furthermore underscores the need to identify new cell-specific markers.

Table 1-1. Cell surface molecule expression in hBM-MSC cultured in FBS and AS (Reprinted with permission from Jan Brinchmann).

CD	Name or marker specificity	FBS	AS
CD13	Metallproteinase	+	+
CD14	Monocyte marker	-	-
CD34	HSC marker	-	-
CD36	Phagocytosis, cell adhesion	-	+/-
CD44	H-CAM	+	+
CD45	Hematopoetic cells	-	-
CD49a	VLA-1α chain	(+)	(+)
CD49d	VLA-4α chain	-	-
CD54	ICAM-1	+/-	(+)
CD58	LFA-3	+/-	(+)
CD62L	L-selectin	-	-
CD71	T9, Transferrin	-	-
CD90	Thy-1	+	+
CD105	Endoglin, SH2	+	+
CD106	VCAM-1	+/-	+/-
CD117	Sca-1	-	-
CD133	HSC marker	-	-
CD152	CTLA-4	-	-
HLA-class I	All nucleated cells	+	+
HLA DR	Antigen presenting cells	-	-
	NGFR	+/-	+/-

+ denotes marker expression on 90% of the cells

(+) denotes marker expression on >10% but <90% of the cells

+/- denotes marker expression on >2% but <10% of the cells

- denotes marker expression on <2% of the cells

1.5.5 hBM-MSC self-renewal and maintenance

Self-renewal refers to the mechanisms that preserve the undifferentiated state of the cells, and is necessary to maintain the stem cell pool. In this way, self renewal ensures that the tissues always have a reservoir of stem cells in case of cell death, disease, or injury. A complex interplay between intracellular signals and extracellular signals *in vivo*, provided by the stem cell niche, regulates self-renewal and differentiation. Understanding the genes and signal transduction pathways that regulate stem cell function is crucial in order to apply these cells for clinical purposes.

Recently, researchers have tried to identify a common pool of genes that underlie the stem cell phenotype by comparing global gene expression in different stem cells. Most of the gene expression profiling has been performed using ESC, hematopoietic stem cells (HSC), neural stem cells (NSC), and skin epithelial stem cells (SESC)[56-61]. These studies have provided

valuable knowledge about the molecular mechanisms that regulate self-renewal and maintenance, but there are inconsistencies between the results, and many questions remain unanswered. Self-renewal and maintenance of hBM-MSC has been less well studied compared to other stem cells. However, promising results have given some insights in the understanding of how hBM-MSC self-renew. Different cytokines and proteins including Wnts[62-65], the Wnt signaling inhibitor Dickkopf-1[66], and tumor necrosis factor-α (TNFα)[67] have all been demonstrated to be involved in hBM-MSC self-renewal. The Wnt, Notch, bone morphogenetic protein (BMP) and the Hedgehog signaling pathways[68, 69] are known to play roles in self-renewal and differentiation in other stem cells, and most likely these pathways also have an important role in the regulation of hBM-MSC self-renewal. Oct-4, Sox2 and Rex1, the transcription factors associated with pluripotency and self-renewal of ESC, are also expressed in hBM-MSC[70]. Another transcription factor, Nf-κB, has been shown to inhibit hBM-MSC differentiation and may also be important for self-renewal[71]. Understanding the exact involvement of the cytokines and their respective signaling pathways, as well as the function of the transcription factors, is difficult and far from accomplished due to their redundancy and the crosstalk between signaling pathways.

1.5.6 hBM-MSC differentiation

Differentiation is the process whereby an unspecialized cell (stem cell) develops into a specialized cell such as a chondrocyte, adipocyte, or osteocyte. Different signals in the surroundings of the unspecialized cell induce expression of a specific set of genes that determine what kind of cell that it will develop into. For a long time it was believed that hBM-MSC, and other ASC, were restricted to form only the cell types of the tissue/organ from which they originated and that differentiation proceeded in one direction only with the cells becoming gradually more restricted with each step. If this is true, stem cells are committed to differentiate when they receive the appropriate signal and can not go backward in development. However, evidence has suggested that cells may not be as irreversibly committed to differentiation along a specific developmental lineage as first believed[49, 50, 72-74]. There are some possible explanations as to how hBM-MSC (or other ASC) can generate differentiated cells beyond their tissue boundaries. Figure 1-6 explains how this may happen.

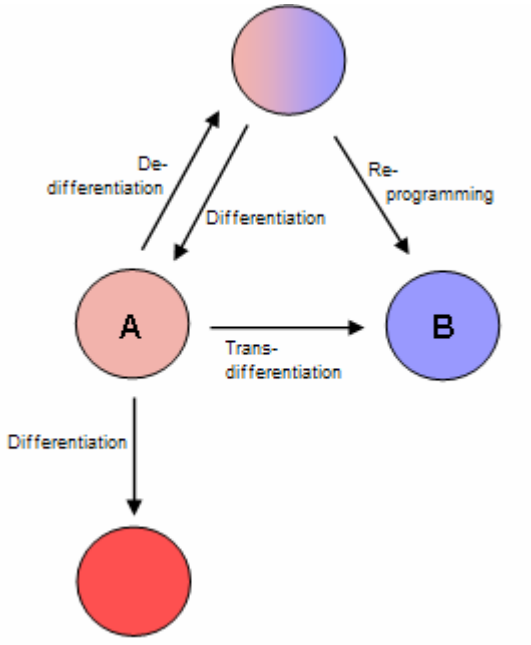

Figure 1-6. The figure shows an imaginary situation where cell A is a progenitor cell for one lineage (for example mesenchymal lineage) and cell B is a progenitor cell for another lineage (for example hematopoietic lineage). Early in development cell A and B had a common ancestor before they separated and developed further. The two-coloured (light pink and blue) cell represents this common ancestor. In the traditional view cell A can differentiate to cells of their own lineage (pink cell). If cell A is capable to differentiate to another lineage there are two possibilities of how this can be done. First, epigenetic modifications can switch the fate of cell A so it can directly develop to cell B. This situation is referred to as transdifferentiation. The other possibility is that cell A can go back to an earlier stage in development, to the stage where it adopts the properties of the common ancestor and then it can develop to cell B by reprogramming of the genome. When a cell reverts to an earlier developmental stage it is called dedifferentiation.(Reprinted with permission from Jan Brinchmann)

If hBM-MSC are to be used in cell therapy it is important to identify and understand the genes that determine hBM-MSC differentiation (and dedifferentiation, transdifferentiation and reprogramming if it happens). Self-renewal and maintenance are closely related to differentiation, thus, it is a very intricate area. The major molecules and signaling pathways that are known to govern the well known trilineage differentiation of hBM-MSC will be briefly described below.

Osteogenesis

Osteogenesis is the formation and development of bone. Runx2 (also known as Cbfa1) and osterix are essential for osteogenesis[75, 76]. They are transcription factors for osteoblast related genes such as collagen type I, osteocalcin and bone sialoprotein. BMPs, especially BMP-6, induce osteoblast differentiation by up-regulation of Runx2 and osterix, which leads to increased production of osteogenic extracellular matrix[77]. The inflammatory cytokine TNF-α work the opposite way by suppressing transcription of Runx2 and destabilizing Runx2 mRNA[67]. Wnt3a, a member (ligand) of the Wnt signaling pathway, suppress osteogenic

differentiation of hBM-MSC when it binds to a G-protein-linked receptor in the so-called canonical Wnt pathway[64], while it induces osteogenic differentiation in the less known non-canonical Wnt pathway[78]. In addition, Wnt signaling interacts with other signaling pathways, such as BMP signaling, to modulate the action of osteogenesis[68].

Chondrogenesis

Chondrogenesis is the formation of cartilage, and depends on several parameters such as cell density, cell adhesion, and the activity of different growth factors. A number of genes have been associated with chondrogenesis, including the transcription factors sox9, sox5, sox6 and scleraxis, the extracellular matrix genes collagen type I, II and IX, aggrecan, decorin, biglycan, cartilage link protein, and cartilage oligomeric matrix protein. These genes are routinely used as positive markers for chondrogenesis, but the molecular mechanism regulating chondrogenesis is generally unknown. Several signaling molecules including members of the Wnt, transforming growth factor β (TGF-β), BMP, and growth and differentiation factor (GDF) families have been shown to stimulate chondrogenesis[79-82]. It has been suggested that downstream mediators of TGF-β and BMP signaling work together to activate genes responsible for chondrogenesis[83]. Various Wnts have different roles in chondrogenesis, for example Wnt1 inhibits chondrogenesis[84], while upregulation of Wnt7a enhances chondrogenesis[85]. On the other hand, sustained Wnt7a expression inhibit chondrogenesis[85].

Adipogenesis

Adipogenesis, or the development of fat, depends largely on the receptor peroxisome proliferator-activated receptor-γ (PPAR-γ)[86-88] and the C/EBP family of transcription factors[89]. Also Wnt signaling plays a role during the adipogenic process. It prevent differentiation of preadipocytes to adipocytes through inhibition of PPAR-γand C/EBP-α[90]. Other interesting examples of adipogenic regulation are the ability of cell shape/cytoskeletal tension and tension-responsive proteins to regulate adipogenesis. It has been demonstrated that cell density, which affects cell shape and cytoskeletal tension, is a key regulator of hBM-MSC commitment to the adipocyte lineages[91].

1.6 Other areas of hBM-MSC biology

Recently, other areas of hBM-MSC biology, such as trophic effects, immunoregulatory functions and homing have received a lot of attention. Most of these research areas are in their very infancy, and will only be described briefly.

hBM-MSC as trophic mediators

Although hBM-MSC can provide cells for cell therapy, they also secrete various cytokines and growth factors that can influence cells in their vicinity [92]. These factors can have several effects such as immunoregulatory effects (see below), inhibition of apoptosis and scar formation, stimulation of angiogenesis (formation of blood vessels) and mitosis, and differentiation of other stem cells[93, 94]. Thus, hBM-MSC can influence tissue regeneration without differentiating into tissue-specific cells themselves[10]. This influence is called trophic or paracrine effect[95] and may have potential applications in cell therapy.

Immunoregulatory function of hBM-MSC

Immunoregulatory effects of hBM-MSC can be considered trophic because cytokines and growth factors play a key role in this context[55]. However, it is mentioned separately from trophic effects because it has attracted tremendous interest recently. Normally, when mismatched cells (allogeneic cells) are transplanted to a host, the transplanted cells will be deleted by the host immune system[96, 97]. There is evidence that hBM-MSC avoid immune recognition and can inhibit different immune responses when transplanted[52, 53, 98, 99]. Furthermore *in vitro* studies also support the immunosuppressive role of hBM-MSC[10, 55, 100, 101]. Thus, hBM-MSC have potential applications in allograft transplantation.

Homing

Homing is the migration of hBM-MSC to various organs in the body. In case of injury or disease, signaling to the hBM-MSC niche is required for homing of hBM-MSC to the site of injury and differentiation to the cell type required for replacement. Several *in vivo* studies, where hBM-MSC have been administered intravenously, show that hBM-MSC engraft into the injured/diseased tissue[21, 23, 102, 103]. The molecular mechanism regulating hBM-MSC homing is poorly understood, but is thought to be a multistep process involving many different surface antigens, cell adhesion molecules, chemokines, cytoskeletal proteins, cytokines, growth factors, and proteolytic enzymes[104-106].

1.7 Project background

1.7.1 Gas tension in the bone marrow

The hBM-MSC niche encompasses all the elements in the surroundings of the hBM-MSC when they are in their native state. There is almost no information about the hBM-MSC niche, but it is expected that hBM-MSC can intermingle not only with each other, but with other cells, including HSC, adipocytes, osteoblasts, endothelial, and stromal cells, as well as extracellular matrix and soluble factors secreted by the cells[107]. An important factor contributing to the hBM-MSC niche is gas tensions. The bone marrow is well circulated due to many small blood vessels (called sinuses) that perforate much of the bone marrow cavity enabling efficient gas exchange between cells and the environment. All the components in the hBM-MSC niche can alter the signaling pathways controlling self-renewal and differentiation. Thus, when investigating hBM-MSC it is important to consider the influence from the *in vivo* environment of the cells, such as the effect of different gas tensions.

Traditionally, the term normoxia refers to the O_2 tension in the incubators, which is approximately 19.7 kPa, or 20 %. Hypoxia refers to O_2 levels which are lower than normoxia [108-110]. In this thesis, however, the term normoxia is used for the O_2 tension surrounding the cells *in vivo*, since these conditions constitute the normal state for these cells. When the cells are removed from the body, they are introduced to unusually high O_2 levels, and these conditions will in this thesis be termed hyperoxia. Hypoxia would then be O_2 levels that are lower than normoxic conditions *in vivo*.

hBM-MSC are adapted to the gas tensions found in the bone marrow microenvironment *in vivo*. At present, it is not possible to accurately measure gas tensions and their spatial variations in the bone marrow. However, the mean normal oxygen tension have been estimated to be between 5% and 9 %[111-113] (normoxia), which is quite similar to that of many other tissues. Standard incubator gas tensions corresponding to 20% O_2 and 5% carbon dioxide (CO_2) are routinely used for *in vitro* expansion of hBM-MSC, and it is being overlooked that such conditions provide O_2 levels that exceed the physiological O_2 tension found in the bone marrow microenvironment. Thus, the cells are exposed to much higher O_2 tensions than under physiological conditions. The effect of this hyperoxia is unknown, but oxygen free-radicals or reactive oxygen species (ROS) could potentially damage key

molecular constituents of the cells[114, 115]. The formation of ROS is a normal consequence of essential biochemical reactions, and most cells and organisms have evolved mechanisms against its toxic effect in their normoxic state. However, when cells are removed from their *in vivo* environment and introduced to hyperoxia *in vitro*, it is possible that these mechanisms are inadequate to protect the cells.

CO_2 is another gas that also may influence the behaviour of hBM-MSC. The CO_2 tension in the bone marrow is unknown, but it is not unreasonable to assume that it is in the range between 5% and 8 %, the same as in many other tissues (Mirtaheri, P. unpublished data). Thus, it is possible that cells would behave more naturally at *in vitro* oxygen tensions lower than 20% and CO_2 tensions higher than 5%.

1.7.2 Motivation for the project

Verfaille *et al*. showed that certain clones of rat MSC-like cells, called multipotent adult progenitor cells (MAPC), showed pluripotency when expanded in an atmosphere of 5% O_2, and a serum concentration of 2%[116]. The cells were plated at low densities, approximately 300 cells/cm^2. Under these culture conditions, the cells had high expression of *OCT-4* which is used as a marker for pluripotent ESC. However, when transferred to hyperoxia (20% O_2) the cells lost *OCT-4* expression and could never retain it. Thus, the low O_2 tension was a requisite for pluripotency of these clones. Because of its association with pluripotency, it is desirable to have increased *OCT-4* mRNA levels in multipotent stem cells as well. This is an indication that the cells are in a more immature, and undifferentiated state.

1.7.3 Isolation of hBM-MSC

Traditionally, hBM-MSC are isolated from the bone marrow-mononuclear cell (BM-MNC) fraction based on their adherence to plastic surfaces. A disadvantage with this method is the undesirable contamination of hematopoietic cells, such as adherent $CD14^+$ monocytes. Enrichment of hBM-MSC can be achieved partly by depleting monocytes from the BM-MNC fraction before culturing the cells, and by expanding and passaging the cells. Previous observations from Dr. Brinchmann's laboratory indicate that there is a difference in monocyte contamination when expanding the cells in FBS and AS: more monocytes adhere to the

culture substrate when expanding the cells in FBS. Therefore, it is possible that depletion of $CD14^+$ cells is unnecessary when using AS as serum supplement. This would facilitate the isolation procedure, and less stress would be exerted on the cells.

1.8 Aims of the study

Based on the results from Verfaillie *et al*, this study aimed at examining the *in vitro* effects of different incubator gas tensions on polyclonal hBM-MSC populations. To do this, hBM-MSC were cultured in six different gas tensions (table 2-1, page 36), and the following aims were pursued:

1) To assay the proliferative capability of hBM-MSC cultured in the different gas tensions.
2) To compare expression of specific genes, which are known to regulate self-renewal and differentiation in ESC.
3) To compare differences in global gene expression.

Due to the observed decrease in monocyte contamination when expanding hBM-MSC in AS, this study also aimed at testing if depletion of monocytes was necessary when AS was used as serum supplement.

2. Materials and methods

2.1 Theoretical background

2.1.1 Bone marrow mononuclear cells

The first step in isolation of hBM-MSC from bone marrow is to isolate BM-MNC. This procedure is based on a gradient centrifugation method developed by Arne Bøyum in 1968[117] (figure 2-2).

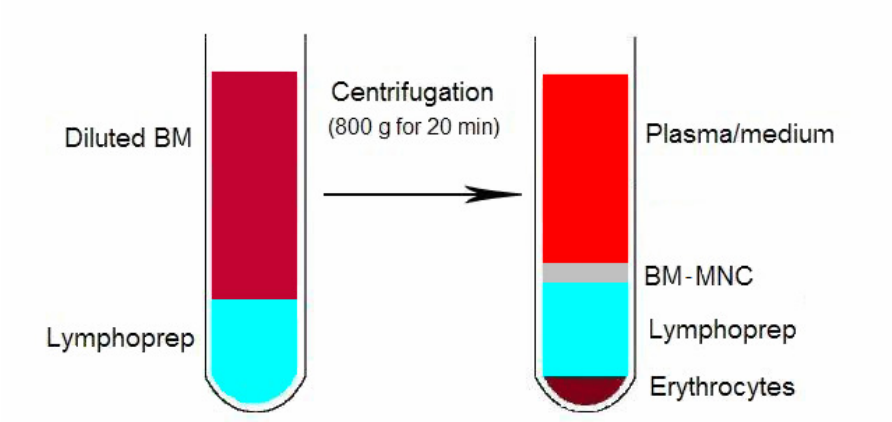

Figure 2-2. After centrifugation at 800 g for 20 minutes four distinct layers are formed. The BM-MNC fraction is the greyish layer between the plasma/medium and the Lymphoprep. See text for details.

The bone marrow aspirate is first diluted in medium (or physiological saline) and then added carefully on top of a centrifugation medium called Lymphoprep, which has a density of 1.077 g/cm^3, followed by centrifugation. Cells in the bone marrow have different densities, and the cells with a higher density than 1.077 g/cm^3 will go through the Lymphoprep and to the bottom of the centrifugation tube (erythrocytes and granulocytes), while the cells with a lower density (BM-MNC) will stay on the top of the Lymphoprep.

2.1.2 MACS® Cell Separation technology

MACS technology is one of the standard methods for cell separation. It is based on three components: MACS microbeads, MACS columns and MACS separators. MACS microbeads are small dextran particles (~50 nm in diameter) with an iron core that are coupled to highly specific antibodies that bind to specific structures on the surface of specific cell types (directly or indirectly). The separation process takes place within a MACS column that is placed in a MACS separator, a strong magnet. The column consists of an iron matrix which, when the

magnet separator is applied, provides a magnetic field that retains labeled cells inside the column, while unlabeled cells pass through (figure 2-3).

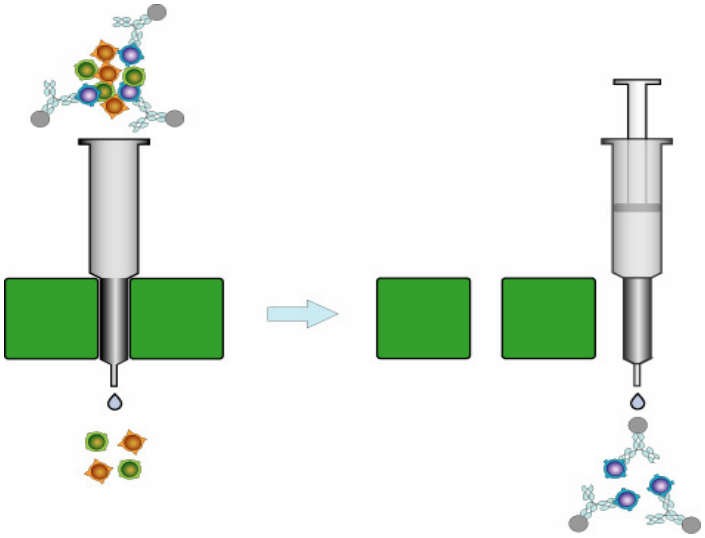

Figure 2-3. To the left: cells are added to a column that is placed inside a magnet. Cells with MACS microbeads coupled to them (blue cells) are retained inside the column because of the magnetic field, while unlabeled cells are passed through and can be collected (negative selection). To the right: the column is taken out of the magnet, medium is added, and a piston is used to elute the labeled cells (positive selection) (Reprinted with permission from Tor Lea).

If the unlabeled cells are collected for use, a negative selection has been performed. Alternatively, if the desired cells are those retained inside the column (labeled cells), they can be eluted and collected for use. This is called a positive selection.

There is no need to remove MACS microbeads from cells after separation because they are biodegradable. They are not known to interfere with structure, activity or function of the labeled cells, and they are too small to interfere with the fluorescence signal used in flow cytometry. Hence, they are compatible with flow cytometry analysis, microscopic analysis, molecular biology experiments, cell culture and *in vivo* experiments.

2.1.3 Nanodrop® ND-1000 Spectrophotometer

Nanodrop® ND-1000 is a spectrophotometer that measures sample sizes as low as 1µl. The sample is placed between two pedestals that employ surface tension to hold the samples in place, and a pulse of xenon light is passed through the sample. The light passing through the sample is analyzed by a spectrophotometer and special software stores the results on a computer. It is sufficient to wipe the pedestal with a dry tissue paper before measuring another sample. Hence, several measurements can be done in seconds with high accuracy and

reproducibility. Nanodrop® ND-1000 can measure absorbance of DNA, RNA, dyes, proteins, and microbial cell culture OD. In this thesis, Nanodrop® ND-1000 was used for measuring RNA concentration and quantifying RNA purity. RNA concentration is calculated automatically by the computer. The ratio of $^{OD260}/_{OD280}$ is used to assess the purity of the RNA. Pure RNA has a ratio of ~ 2.0 (details are described in Nanodrop's ND-1000 spectophotometer V3.3 user's manual).

2.1.4 Agilent® 2100 Bioanalyzer

Agilent 2100 bioanalyzer is a microfluidics platform offering solutions for analysis of DNA, RNA, proteins, and cells. In this thesis the bioanalyzer was used to determine RNA integrity before microarray analysis. The method is based on electrophoretic assays in a chip format containing microchannels and sample wells. During the procedure, the microchannels are filled with a gel containing a fluorescent dye. Once the wells and channels are filled the chip becomes an electrical circuit and the samples are added. Charged molecules are then electrophoretically driven by a voltage gradient. The fluorescent dye will intercalate into the molecules and the complexes will be detected by a laser-induced fluorescent. Data is then translated into gel-like images and electropherograms, and a standard curve is used to determine the migration time and fragment size. Results like sample concentration, and the RNA integrity number (RIN) are stored on a computer. RIN indicates RNA integrity. The RIN software algorithm is based on a numbering system from 1 to 10, with 1 being the most degraded profile and 10 being the most intact (details are described in Agilent 2100 bioanalyzer expert user's guide).

2.1.5 Real-time RT PCR

In this study real-time RT PCR was a central analysis method, and the method is therefore described in detail. Real-time RT PCR is a powerful tool for quantification of nucleic acids because of its high specificity, sensitivity and reproducibility[118]. The process of real-time RT PCR involves four steps: (1) preparation of RNA, (2) reverse transcription (RT) of RNA to complementary DNA (cDNA), (3) amplification of target cDNA by real-time RT PCR, and (4) data analysis[119]. Due to the exponential amplification of target template during PCR, the products generated are directly proportional to the amount of template prior to the start of the

PCR process[119]. In real-time RT PCR it is the initial amount of template that is quantified, rather than the amount of target accumulated at the end of the PCR process as in traditional PCR[119]. During the first PCR cycles the products generated increase exponentially. Thereafter, mainly due to reagent limitations, presence of PCR inhibitors in the samples, and accumulation of inorganic pyrophosphate (released as a result of nucleotide incorporation), the polymerase reaction eventually slows down and the PCR product is no longer being doubled at each cycle (figure 2-4). Therefore, variable amount of PCR product accumulate at the end of the reaction, making traditional PCR unreliable; it gives no information about the initial amounts of target templates that were present in the samples. Hence, traditional PCR can only be used for non-sensitive semi-quantification, or to distinguish a positive sample from a negative sample. Only during the exponential phase, when products are being doubled at each cycle, is it possible to extrapolate back in order to determine the initial amount of template. Real-time RT PCR measures PCR products as they accumulate (in real time) and allows for quantification in the exponential phase and therefore removes the variability associated with traditional PCR[118]. This gives real-time RT PCR a major advantage over traditional PCR. The real-time RT PCR system is based on the detection and quantification of a fluorescent probe that binds to the product formed[118]. The fluorescence intensity signal reflects the amount of PCR product formed, and thereby makes it possible to monitor the accumulation of products as the PCR reaction proceeds. The fluorescence signal is considered a real signal only when it is detected above an arbitrary threshold chosen by the computer. The fractional PCR cycle number at which the fluorescent signal passes the threshold value is defined as C_T and will always occur during the exponential phase during the early cycles of PCR (figure 2-4). The higher the initial copy number of the target template, the sooner a significant increase in fluorescence (lower C_T value) is observed.

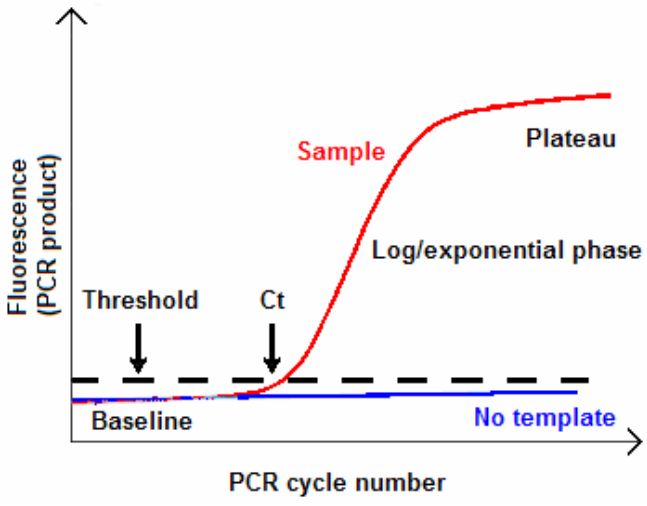

Figure 2-4. PCR amplification plot.
A typical amplification follows the red line, with little change in fluorescence (PCR product) in the initial cycles followed by an exponential growth phase and a plateau phase where amplification decreases. Traditional PCR measures the amount of product generated at the end of the reaction (plateau), while real-time RT PCR measures the amount of product in the exponential phase. Baseline is defined as the initial cycles of PCR in which there is little change in fluorescence signal. Threshold is set to be above baseline and sufficiently low to be within the exponential phase. C_T is the cycle number at which the fluorescence passes the threshold.

Generally two quantification strategies can be performed: absolute quantification and relative quantification (RQ). Absolute quantification determines the exact input copy number of the target template by comparison with standard curves[118]. RQ is also known as the comparative C_T method ($2^{-\Delta\Delta Ct}$). This method determines the change in expression of a target template relative to some reference group (calibrator), such as an untreated control or a sample at time zero in a time-course study[120]. RQ eliminates the need for standard curves and uses mathematical equations to provide accurate comparison between the initial levels of template in samples, without requiring the exact copy number of the template. For most gene expression studies RQ is the most relevant approach. For example, stating that a given treatment increased the expression of a gene by 10 fold may be more relevant than stating that the treatment increased the expression of the gene from 1000 copies to 10000 copies. Thus, RQ was the preferred choice in this thesis.

Certain assumptions and testing of these assumptions are required for RQ data to be valid: (1) a critical step in real-time RT PCR is to find proper amounts of RNA that will be efficiently reverse transcribed to cDNA. The amount of cDNA produced must reflect the amount of RNA input for the results to be sensitive and accurate[121]. This can be tested by making a dilution series of the RNA. After RT, the cDNA is subjected to real-time RT PCR, with all samples amplifying the same target template (preferably a housekeeping gene, see below). If

the amount of RNA input is proportional to the amount of cDNA produced, then the plot of log RNA input versus C_T value will give a linear curve. Then it is safe to use these amounts of RNA in the RT reaction. If too much RNA is loaded into the RT reaction, not all RNA will be copied to cDNA due to lack of reagents and presence of RT inhibitors in the sample material. This will give a falsely high C_T value which will not correspond with the linear curve.

(2) In gene expression experiments, the real-time RT PCR is normalized for the amount of RNA added to the RT reaction by an internal RNA reference gene, which is a cellular RNA that is amplified simultaneously with the target. The accuracy of the normalized data is highly dependent on the reliability of the internal reference[120]. Therefore, their expression levels should be expressed at constant levels in different experimental conditions. The most common genes used for normalization are housekeeping genes like *GAPDH*, *18S rRNA* , *β_2-microglobulin* and *β-actin*. However, none of these internal references are ideal. All have been shown to be modified by different experimental treatments[122]. Therefore, it is highly recommended that the internal reference gene is validated for each experiment to determine that gene expression is unaffected by the experimental treatment[120]. This can be performed by using a modified version of the $2^{-\Delta\Delta Ct}$ method called $2^{-\Delta C't}$ [120]. In this situation, normalisation must be carried out to some measurement external to the real-time RT PCR experiment. The most common method is to use UV absorbance to determine the amount of RNA added to each RT reaction. Real-time RT PCR is then set up using cDNA derived from the same amount of RNA input for all samples.

(3) The amount of target template in a sample is given by $2^{-\Delta\Delta Ct}$ (derivation of this equation is described in Applied Biosystems User Bulletin No. 2 (P/N4303859)), where $\Delta\Delta C_T = \Delta C_T$ (sample) - ΔC_T (calibrator), and ΔC_T is the C_T value of the target gene subtracted from the C_T value of the internal reference gene that is amplified simultaneously as the target gene. This calculation is the basic principle of RQ, and is only valid if the amplification efficiency of the target template and the internal reference is approximately equal (above 90 %)[118]. This can easily be assessed by looking at how ΔC_T varies with template dilution. A plot of the log RNA input versus ΔC_T is made and if the slope of the regression line is close to zero (between 0.1 and -0.1), the amplification efficiency of the two is similar enough, and RQ can be used.

2.1.6 Microarray technology

Microarray enables gene expression measurements of thousand of genes in a single sample. Although relatively new, this method has been proven to be extremely useful within molecular biology. In this type of analysis, most of the genes of an organism are represented by oligonucleotide, cDNA, or DNA sequences (probes) that are spread out on a high-density array. The array contains several thousand of spots and each spot consist of hundreds of thousand identical probes that represent one gene (one gene may be represented by many spots). Usually, mRNA from cells, or tissues, is reverse transcribed to cDNA and labeled with a fluorescent dye. The labeled cDNA is then applied to the array and because of the hybridization property of nucleic acids, any sequence that finds a complementary strand will bind to a specific spot (figure 2-5) and a fluorescent signal is created[123].

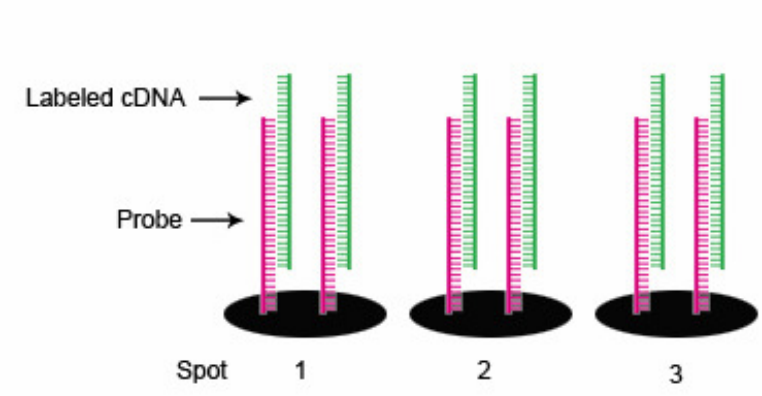

Figure 2-5. Labeled cDNA hybridize to their complementary probe. For simplicity, only a few probes and spots are shown. See text for details.

The signal is picked up using a scanner and a computer determines the amount of sample bound to each spot on the array. The amount of fluorescence is assumed to be proportional to the amount of each mRNA in the original biological sample. There are many possible sources of errors in microarray analysis, such as variation within and between oligonucleotide spots, efficiency of dye-incorporation, hybridization efficiency, and accuracy and fluctuations in scanning the fluorescent signals[123]. There are many statistics and data analysis tools available for processing these variations[123]. It is important to use these tools carefully and to process and analyze the data while keeping the sources of variations in mind. Several types of microarray technologies (platforms) for measuring gene expression are availible[124]. In this thesis the beadarray technology from Illumina was used.

2.1.7 Illumina's BeadArray technology

Conventional microarrays are manufactured by spotting or synthesizing probes onto a solid phase at known locations[125]. In contrast, the beadarray technology involves random assembly of 3 micron silica beads into wells that have been etched into the surface of the array (figure 2-6).

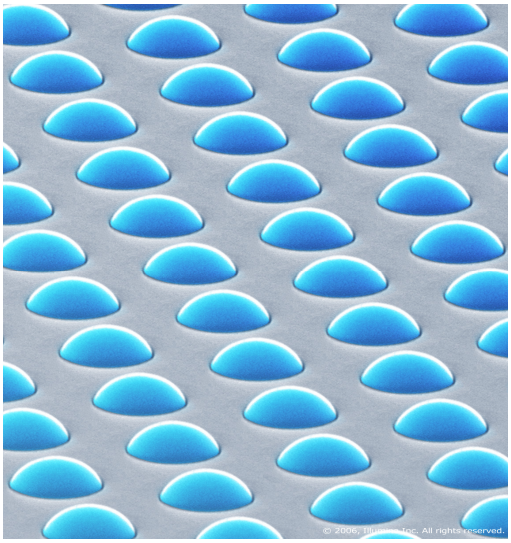

Figure 2-6. A pool of 3 µm silica beads is loaded by a self-assembly process into the microwells in the beadchip. Each bead is represented on the beadchip ~ 30 times. (Reprinted with permission from Illumina).

Each bead is covered with hundreds of thousand copies of a specific oligonucleotide consisting of a 50 bp probe and a 29 bp address sequence. The probe acts as the capture sequence and the address sequence acts as a decoding sequence that enables the identification and location of the bead on the array (figure 2-7).

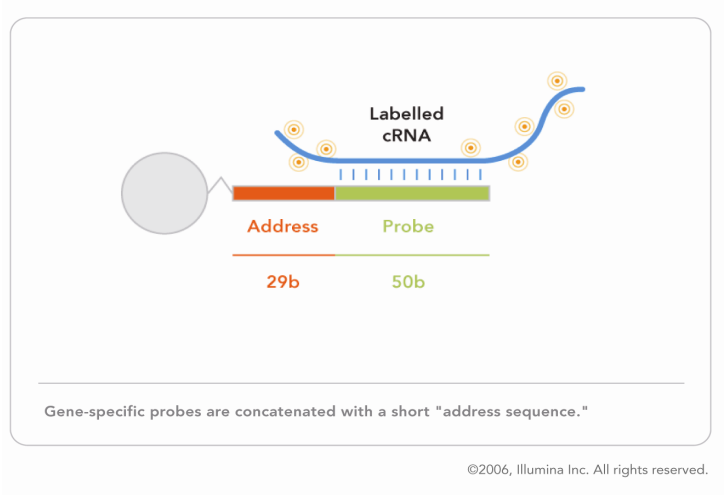

Figure 2-7. Each bead is coated with hundreds of thousands copies of the same probe, to which labeled cRNA can hybridize. Concatenated to the probe is a short address sequence, which is used to identify the bead. (Reprinted with permission from Illumina).

The address sequence is designed such that it has no sequence homology to genomic sequences within the genome to be studied. The decoding process is based on several sequential hybridizations of a few dye-labeled oligonucleotides to the address sequence. An algorithm then identifies the probe and its location by tracking the oligonucleotides hybridizing to the address sequence[126]. Each bead type is represented on the surface of the array an average of more than 30 times. This redundancy results in high data quality, because each signal created during hybridization is based on the average of many independent readings. It also enables the removal of outliers without affecting the overall results. Randomly assembled bead assays results in very high density (~40,000 times higher than a typical spotted array) which gives small assays and, therefore, very small volumes of sample and reagents are needed. Briefly, the process of whole genome gene expression using the Illumina beadarray technology can be divided into four steps: (1) sample preparation, (2) sample hybridization, (3) scanning and (4) data analysis. Because of the many possibilities of errors during the microarray procedure, seven control categories are built into the beadarray system. These controls cover every aspect of an array experiment from the biological specimen, to sample labeling, to hybridization, signal detection, and negative controls that defines the system background (details are described in the "Whole-Genome Gene Expression for Beadstation" user manual from Illumina).

2.1.8 Genespring GX 7.3.1

The Genespring software provides statistical tools for fast visualization and analysis of microarray data. It is easy to use and designed specifically for the needs of biologists. Genespring enables visualization of expression data using a wide range of graphical displays such as 2D and 3D scatterplots, chromosome maps, box plots, and pathway diagrams. Using Genespring it is easy to identify target genes and their function, assess changes in gene expression, determine if a particular gene is a member of a known pathway, create annotated lists of genes identified through graphical tools, uncover statistically meaningful data, create experiments that link the expression data to a variety of parameters, and ensure data quality with powerful statistical tools and normalization methods. (For details: www.agilent.com/chem/informatics).

2.2 Adjustment of the incubators

One week before the experiment started six different incubators were adjusted with the gas tensions shown in table 2-1, and with a temperature of 37°C, and 92 % humidity.

Table 2-1. Different incubator gas tensions used for culturing hBM-MSC.
Gas tension 1 is standard incubator air

	O_2	CO_2
1.	20 %	5 %
2.	20 %	7.5 %
3.	6 %	5 %
4.	6 %	7.5 %
5.	9 %	5 %
6.	9 %	7.5 %

2.3 Preparation of autologous serum

Venous blood (450 ml) from the bone marrow donor was drained into blood bags. The blood was then transferred quickly to 10 ml vacutainers without anticoagulants, and allowed to clot for 3-4 hours at 4°C. After clotting, the blood was centrifuged at 1800 x g for 20 minutes at 4°C, and serum was collected. Subsequently, the AS was passed through a 0.45 µm pore size filter, and then through a 0.20 µm pore size filter. Aliquots of the sterile AS were stored at -20°C.

2.4 Isolation and culture of hBM-MSC

2.4.1 Isolation of BM-MNC

Syringes were coated with monoheparin (to avoid coagulation) and used to obtain between 50-90 ml bone marrow aspirate from the iliac crest of each of six donors after informed consent. The bone marrow aspirate was quickly diluted 1:3 in basal medium (D-MEM/F12 (1:1) + Glutamax from Gibco) supplemented with 100 units/ml penicillin, 100 µg/ml streptomycin and 2.5 µg/ml amphotericin B. The diluted aspirate was then added carefully to 50 ml tubes containing 15 ml Lymphoprep and centrifuged at 800 x g for 20 minutes, without breaks. After centrifugation, the layer containing the BM-MNC was collected in new tubes and washed twice with medium at 300 x g for 10 minutes. Pellets were resuspended, pooled in a new tube, and the cells were counted. The BM-MNC fraction from donor 1, 2, and 3 was

depleted of $CD14^+$ cells before being established in culture, while the BM-MNC fraction from donor 4, 5, and 6 were established directly in culture.

2.4.2 Use of MACS® Cell Separation system

The MACS system was used to test out the necessity of removing adherent $CD14^+$ monocytes from the BM-MNC fraction. Cell separation was performed using protocols and reagents from the manufacturer. Briefly, the cells from donor 1, 2, and 3 were washed in "superMACS buffer" and labeled with MACS microbeads coupled to mouse anti-human CD14 monoclonal antibody. Subsequently, the cells were added to a column inside a magnet and a negative selection was performed. The $CD14^-$ cells passed through the column and were collected for further use, while the $CD14^+$ cells were retained inside the column. The CD14- cells were counted and seeded out in culture flasks.

2.4.3 Culture of hBM-MSC

The cells were allowed to adhere overnight. At day 1, non-adherent cells were discarded, and adherent cells were washed three times with 30 ml medium and cultured in fresh culture medium. Culture medium was replaced every 3 or 4 days until 40-50 % confluence was reached. Subsequently, cells were detached using trypsin EDTA and replated at 3000 cells/cm^2. Cells were cultured for three passages and cell pellets for real-time RT PCR and microarray analysis were made at passage 2 and 3. The rest of the cells were frozen down as living cells. The culture medium consisted of D-MEM/F12 supplemented with 10% or 20% AS, 100 units/ml penicillin, 100 µg/ml streptomycin, and 2.5 µg/ml amphotericin B. Amphotericin B and 20% serum were used in the culture medium until the first passage. After the first passage amphotericin B was removed, and 10% instead of 20% AS was used for further cell cultures. Culture media were always pre-incubated in their respective incubator, without AS, for at least 2 hours before use. AS was always added at the same time as the cells. Pre-incubation of the culture medium was done in an attempt to reach equilibrium between O_2 and CO_2 in the gas and the liquid phases before adding the cells. Previous results have shown that it takes 2 hours to establish equilibrium between the gas and the liquid phases when the height of the medium is 4 mm (unpublished data from Dr. Brinchmann's laboratory). This height corresponds to the amount of culture medium used in this study. It

was decided not to include AS in the culture medium during pre-incubation. The reason is that AS contains factors that are important for the attachment of the cells to the plastic surfaces, and pre-incubation with AS may influence the attachment of the cells in an unknown way. Experiments have indicated that less hBM-MSC attach to the culture surface when pre-incubating medium with AS (unpublished data from Dr. Brinchmann's laboratory).

Trypsination – detachment of the cells

Detachment of the cells was performed according to protocols from the manufacturer. Briefly, the used culture medium was transferred to a sterile tube, and the monolayer of cells was washed with trypsin to remove all traces of serum. New trypsin was added, and the flask was incubated at 37^{o}C until all cells had detached from the surface. The trypsin containing the cells was then transferred to the used culture medium in order to inactivate the trypsin. Cells were then centrifuged at 300 x g for 10 minutes. The pellet was resuspended in fresh culture medium, and cells were counted and seeded in new culture flasks.

Counting cells

Cells were counted using a KOVA chamber according to protocols from the manufacturer. Briefly, 18 µl cell suspension was mixed with 2 µl ethidium bromide/acridin orange and transferred to the KOVA chamber. Cells were visualized and counted using a fluorescence microscope.

Freezing down living cells

The freeze down medium, consisting of D-MEM/F12 supplemented with 20% AS and 5% DMSO, was mixed and filtered through a 0.25 µm pore size membrane. Cells were centrifuged at 300 x g for 10 minutes in culture medium. Pellets were resuspended in 1 ml freeze down medium, transferred to cryotubes (1.5 ml) and quickly transferred to -70^{o}C for storage. This rapid freeze down technique has been shown to yield cells with at least the same viability as the more elaborate technique of gradually adding DMSO-containing medium (unpublished data from Dr. Brinchmann's laboratory).

Freezing down pellets

Approximately 1 – 2 x10^{6} cells from passage 2, and 3 were centrifuged in RNase free Eppendorph tubes at 320 x g for 2 minutes, supernatant was discarded and the pellets quickly transferred to liquid nitrogen. Pellets were then stored at - 70^{o}C.

2.5 RNA isolation and DNase treatment

RNA was isolated using the RNaqueous®-4 PCR Kit from Ambion (Ambion, Austin, TX). All materials and solutions were supplied with the kit. Briefly, 1 – 2 x10^6 cells from passage 2 were homogenised in lysis solution. The cell lysate was applied onto a filter cartridge column and DNA, proteins, tRNA, and other debris were washed away using two different washing solutions. Subsequently, RNA was eluted from the column followed by DNase treatment to ensure removal of contaminating DNA. RNA concentration and RNA integrity was assessed before storing RNA at -70^{o}C.

2.6 RNA measurements and RNA integrity

2.6.1 Determining RNA concentration and RNA purity

RNA concentration was measured with the Nanodrop® ND-1000 Spectrophotometer following protocols supplied by the manufacturer. Briefly, before start-up the pedestal surfaces were cleaned to remove dirt and prevent sample carry-over that can cause erroneous absorbance readings. The program ND-1000 3.2.0 was opened and RNase free water was added on the pedestals to initialize the spectrophotometer. Before starting the measurements, the spectrophotometer was blanked. RNA concentration and RNA purity were determined by analyzing 2 µl RNA solution. The results were stored on the computer.

2.6.2 RNA integrity

In Dr. Brinchmann's laboratory, RNA integrity is routinely checked by electrophoresis on a 1% agarose gel. At the Microarray core facility at Rikshospitalet - Radiumhospitalet they use the Agilent® 2100 Bioanalyzer system to check RNA integrity. It is always recommended that RNA integrity is checked before starting analysis such as real-time RT PCR and microarray. Therefore, RNA integrity was checked by two different methods in this thesis: on elecrophoresis before real-time RT PCR analysis, and by the Agilent® 2100 Bioanalyzer system before microarray analysis.

Agarose gel electrophoresis of RNA

0.5 g agarose powder was added to 50 ml TAE and heated in the microwave oven. After cooling, a drop of ethidium bromide was added and the solution was poured into a mould. Approximately 700 ng RNA was mixed with 0.5 X formadide loading dye and set to

incubation at 70°C to denature the RNA. After denaturation the samples were added to the gel, and separation was performed at 80 V for 30-40 minutes. Finally, UV-light was used to visualize the separated bands and pictures were taken.

Agilent® 2100 Bioanalyzer

Evaluation of RNA integrity using the Agilent Bioanalyzer was performed at the Microarray core facility at Rikshospitalet-Radiumhospitalet, using the Agilent Bioanalyzer 2100 RNA 6000 Nano assay following protocols from the manufacturer. Briefly, the gel-dye mix was prepared and loaded into the chip. Subsequently, sample buffer, ladder and the sample were loaded into the wells and the chip was run in the Bioanalyzer.

2.7 cDNA synthesis for real-time RT PCR

Reverse transcription was performed using the High Capacity cDNA Archive Kit from Applied Biosystems (Applied Biosystems, CA, USA) according to protocols from the manufacturer. Half amount of reagents was used, and all reagents were supplied with the kit. Briefly, 200 ng RNA was diluted with RNase free water and mixed with pre-made mastermix in a total volume of 50 µl. Reverse transcription was performed on the Geneamp® PCR system 9700. Thermal parameters were 25°C for 10 minutes followed by 37°C for 120 minutes. cDNA was stored at -20°C before use.

2.8 Real-time RT PCR

Real-time RT PCR analyses were performed on the 7300 Real-Time RT PCR system from Applied Biosystems using reagents and following protocols from the Taqman® Gene Expression Assay Protocol (Applied Biosystems).

2.8.1 Gene expression analysis

Taqman assays for the following target genes were selected: *OCT-4, SOX2, NANOG, KLF4, and C-MYC* (see table 2-2 for assay ID details). Briefly, 6 µl cDNA was mixed with "Taqman Universal PCR Mastermix 2X (No AmpErase UNG)", RNase free water, and "Taqman gene expression assay" according to ratios described in the protocol. The mix was transferred to a 96-well plate, and RQ was performed using the 7300 System SDS software. The thermocycler

parameters were 95°C for 10 minutes followed by 40 cycles of 95°C for 15 seconds and 60°C for 1 minute. All samples were run in triplicates. Following the instructions in the protocol and using 6 µl cDNA in the set up, the RNA input for every replicate corresponds to 6 ng. To check for possible contamination, RNA and water were used as controls. All samples were scaled according to the expression level of standard incubator air (20% O_2, 5% CO_2 - calibrator).

Table 2-2. Assay ID for targets used in Real-time RT PCR.

Target	Assay ID
OCT-4 (POU5F1)	Hs00742896_s1
SOX2	Hs00602736_s1
NANOG	Hs02387400_g1
C-MYC	Hs00153408_m1
KLF4	Hs 00358836_m1
GAPDH	Hs 00266705_g1

Before the gene expression analysis was performed, the efficiency of the RT reaction, validation of the internal reference gene, and the amplification efficiency of the targets and the internal reference were examined.

2.8.2 Efficiency of RT

To find an amount of RNA input that was proportional to the amount of cDNA produced in the RT reaction, a 2-fold dilution series of RNA was made. The least concentrated sample contained cDNA derived from 0.9 ng RNA, and the most concentrated sample contained cDNA derived from 15 ng RNA. cDNA from all samples were amplified using real-time RT PCR, and a plot of log RNA input versus C_T value was produced. To ensure reproducible amplification through all cycles, a highly expressed gene is preferred to be the amplification target in this kind of experiment. Hence, *GAPDH* was chosen as target.

2.8.3 Validation of internal control

GAPDH was chosen as internal reference gene for all experiments. To validate that *GAPDH* was not affected by the different gas tensions the modified version of $2^{-\Delta\Delta Ct}$, $2^{-\Delta C't}$, was applied[120]. This equation enables relative gene expression measurements when only one gene is being studied. Thus, the target gene and the internal reference gene are one and the same.

RNA input corresponding to 6 ng RNA was used as the external measurement for normalisation.

2.8.4 Amplification efficiency

To validate the amplification efficiency, test samples that are known to express the target genes at high levels are required to ensure amplification. Alternatively, a purified PCR product can be used. Embryonic carcinoma cells (ECC) express high levels of all the target genes used in this real-time RT PCR experiment. RNA isolated from ECC was therefore used as test samples for all target genes. A 3-fold dilution series of RNA was made, and real-time RT PCR was set up using cDNA derived from the diluted samples. A plot of template dilution versus ΔC_T was made to assess amplification efficiency. The least concentrated sample contained cDNA derived from 0.025 ng RNA, and the most concentrated sample contained cDNA derived from 6 ng RNA.

2.9 Microarray

2.9.1 Illumina Human-6 v2 Expression Beadchip

Illumina's beadarray technology was used following protocols from the manufacturer. Briefly, RNA integrity was checked and biotin-labeled cRNA was produced by reverse transcription followed by *in vitro* transcription, using the Illumina® Totalprep RNA amplification Kit (Ambion, Inc, Austin, TX). Labeled and amplified cRNA was applied to the Human-6 v2 Expression Beadchip (containing 46718 probes – many duplicates) and allowed to hybridize at 55°C overnight on the BeadChip Hyb Wheel. The following day the Beadchip was washed, blocked, and a signal was developed with streptavidin-Cy3 using FluoroLink™ Cy™3 (Amersham Biosciences, Piscataway, NJ). The Beadchip was then scanned with the Illumina Beadstation 500. The scanned image files were imported into the Illumina Beadstudio software for basic quality control of the data. The resulting data files were exported to Genespring GX 7.3.1 (Agilent Technologies, Santa Clara, CA) for further gene expression analysis.

cRNA amplification was performed at the Microarray core facility at Rikshospitalet-Radiumhospitalet, while hybridization, washing, scanning and Beadchip quality analysis was performed at Service XS in Leiden, the Netherlands.

hBM-MSC expanded in three different gas tensions were analyzed by the Illumina Beadchip system:

1. 20% O_2 and 5 % CO_2
2. 6 % O_2 and 7.5 % CO_2
3. 9 % O_2 and 5 % CO_2

2.9.2 Genespring GX 7.3.1

Briefly, the raw data were normalized by (1) Data transformation: Set measurements less than 10.0 to 10.0, (2) Per chip: Normalize to 50^{th} percentile and (3) Per gene: Normalize to median. The three donors were used as biological replicates and "Gas tension" was used as parameter when creating the experimental design. In order to evaluate the quality of the samples, hierarchical clustering (condition three) was applied. Before starting analysis, scatterplots of the different gas tensions, with 2-fold as cut-off, was applied to obtain a rough and visual overview of the gene expression differences between the gas tensions. Afterwards, genes with large spread (more than one standard deviation from the mean) were removed. Furthermore, genes with less than 1.5-fold change difference across the experiment were excluded. Thereafter, a one-way ANOVA, with a false discovery rate of 0.05, was used to determine genes with statistically differential expression between the different gas conditions. The one-way ANOVA analysis was performed both without and with multiple testing correction. The genes that passed the one-way ANOVA analysis were used to make pairwise comparisons between the different gas tensions. For this purpose volcano plots, with 2-fold difference and 0.05 as P-value cut-off, was applied.

2.10 Statistical analysis

Figures for cell counts and real-time RT PCR data, were created using GraphPad Prism 5. All statistical analysis on the real-time RT PCR data, were performed using Origin 7.5 SR 6 version. A Two Sample t-Test was used to test for significant differences in gene expression compared to the control groups (calibrator).

Figures for microarray data were obtained from the Genespring GX 7.3.1 program. The statistical analysis on the microarray data, were performed using the statistical package integrated in Genespring GX 7.3.1. A one-way ANOVA was used, both without and with the Benjamini and Hochberg multiple testing correction, in order to compare how the different gas tensions affected gene expression.

3. RESULTS

3.1 Depletion of CD14+ cells

The BM-MNC fractions from donor 1, 2 and 3 were depleted of $CD14^+$ cells using the MACS cell separation system. When these cells were cultured after depletion of the CD14+ cells, small round adherent cells were observed during the first week of culturing (figure 3-1), and only few small adherent fibroblast-like cells were observed during the second week.

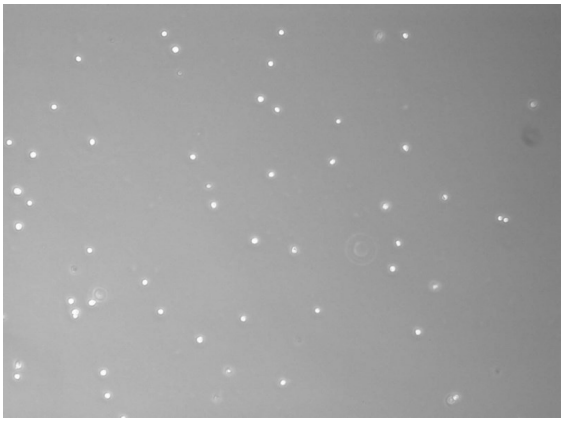

Figure 3-1. Before plating, $CD14^+$ cells were depleted with the MACS system. A representative picture is shown for cells from donor 1 at day 6 in culture. Image magnified 200X.

The BM MNC fractions from donor 4, 5 and 6 were established directly in culture without depletion of CD14+ cells. In these cultures, adherent fibroblast-like cells were observed from day 1, and between day 8 and 12 the cells reached 40% to 50 % confluence, and were ready to be replated. Only minor contaminations of monocytes were observed by a visual assessment of the cell cultures using a light microscope. After replating of the cells, no distinct monocyte contamination was observed in the cultures (figure 3-2). However, visual assessment using a light microscope is a rough method for determining the purity of the cell cultures.

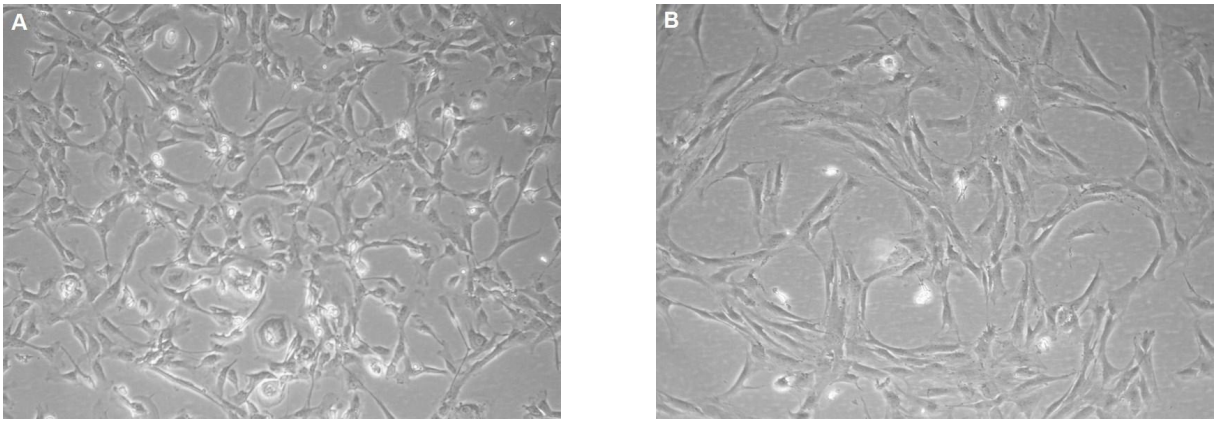

Figure 3-2. Images of cells expanded in 6% O_2 and 5% CO_2 (donor 6). (A) Cells at passage 0, containing monocytes that have a characteristic shape resembling "fried eggs". (B) For cells at passage 1, no distinct monocyte contamination was observed, and the hBM-MSC were larger. The morphology of the cells did not change during passage 1, 2 or 3. Images magnified 200X.

Since the isolation procedure was efficient without depleting $CD14^+$ cells, the hBM-MSC from donor 4, 5 and 6 were used for further experiments.

3.2 Morphology of hBM-MSC

From the first colony formation until the expansion was ended, the hBM-MSC showed the fibroblast-like shape displayed in figure 3-2. No marked alterations in cell morphology (size and shape) were observed between hBM-MSC expanded in the different gas tensions. However, for all gas tensions, the hBM-MSC appeared to be larger and longer in passage 1 to 3 compared to passage 0 (figure 3-2). Although, not clear in the displayed images, a heterogeneous mix of cells was observed in all cell cultures. The majority of the cells appeared thin and spindle shaped, while a minor portion of the cells had a wider cell body containing a more flattened cytoplasm.

3.3 Proliferation capability of hBM-MSC

In order to compare the effect of different gas tensions on the proliferative capability of hBM-MSC, the cells were counted at every passage and plated at a constant density of 3000 cells/cm^2. Growth curves showing the calculated cumulative cell counts between cells expanded in the different gas tensions are shown for donor 4 in figure 3-3.

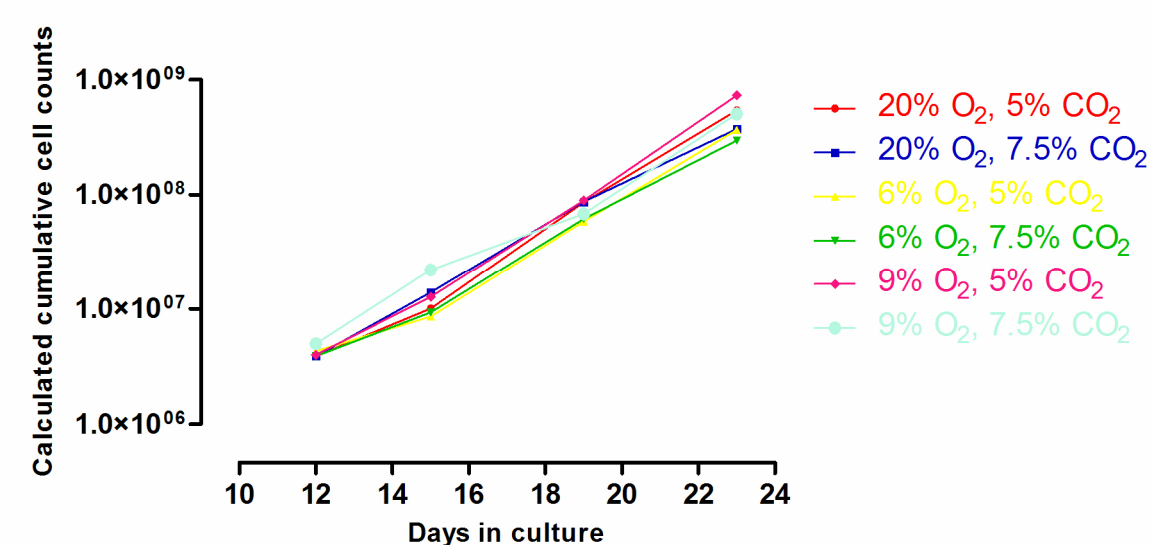

Figure 3-3. Proliferation rates of hBM-MSC (donor 4). hBM-MSC were plated in 175 cm^2 flasks in culture medium at 3000 cells/cm^2 and expanded in the O_2 and CO_2 tensions indicated for up to 23 days. At day 12, the cells were 40% to 50% confluent and were ready to be replated. Hence, the first cell count was performed at day 12.

All donors showed a similar growth pattern, and, the growth curve for donor 4 was therefore considered representative for the three donors. There were no consistent differences in cell counts between hBM-MSC expanded in the different gas tensions.

3.4 Real-time RT PCR

3.4.1 RNA purity and integrity

All RNA samples (isolated from cells at passage 2) were checked for purity and integrity before real-time RT PCR. Table 3-1 shows the results from donor 4, and is representative for donor 5 and 6.

Table 3-1. RNA concentration and $^{OD260}/_{OD280}$.

Donor 4	ng/ul	$^{OD260}/_{OD280}$
20% O_2, 5% CO_2	251.34	2.01
20% O_2, 7.5% CO_2	218.49	2.02
6% O_2, 5% CO_2	215.12	2.06
6% O_2, 7.5% CO_2	225.05	2.09
9% O_2, 5% CO_2	302.32	2.01
9% O_2, 7.5% CO_2	241.09	2.05

All samples had an $^{OD260}/_{OD280}$ ratio of ~ 2.0, thereby indicating pure RNA, and that the samples could be used as templates for real-time RT PCR experiment. The integrity of the RNA samples was furthermore analyzed by agarose gel electrophoresis (figure 3-4).

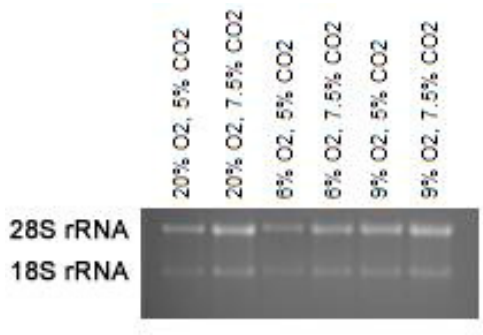

Figure 3-4. 0.5-0.7 µg RNA were run on a 1% denaturing agarose gel in the presence of ethidium bromide. Image is from donor 4, and is representative for donor 5 and 6.

Clear bands, without any smear, corresponding to 28S rRNA and 18S rRNA were observed, indicating that the RNA had not been subjected to degradation.

3.4.2 Efficiency of RT

In order to determine an appropriate amount of RNA input for the real-time RT PCR reactions, the efficiency of the RT reactions using various dilutions of RNA, ranging from 0.9 ng to 15 ng, was assayed, and a plot of RNA input versus C_T was made (figure 3-5).

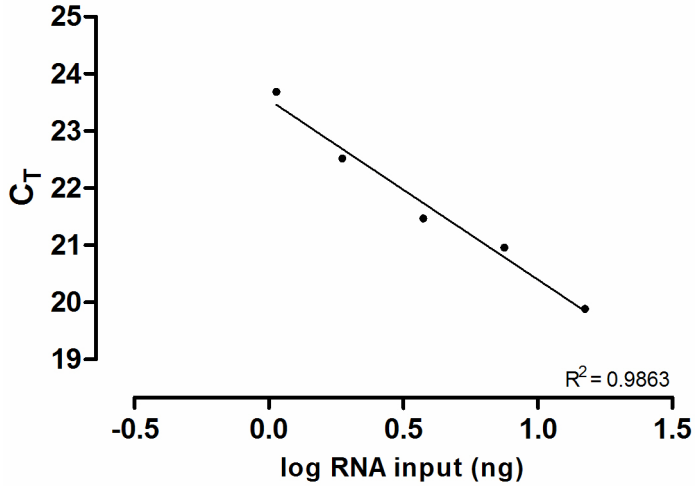

Figure 3-5. A 2-fold dilution series of RNA were made. The real-time RT PCR reactions were set up using cDNA derived from the diluted RNA samples. Data are displayed as mean (n = 3). Standard deviation was too small to be visible in this plot.

The plot gave a linear curve, showing that the cDNA amounts produced were proportional with the amount of RNA input for all dilutions. This experiment demonstrated that all RNA inputs were suitable for real-time RT PCR. Of these concentrations, RNA amounts corresponding to 6 ng was chosen to be used in real-time RT PCR reactions.

3.4.3 Validation of *GAPDH* as internal reference gene

For valid determination of the gene expression levels measured by real-time RT PCR, the expression level of the gene used as an internal reference in the experiments can not be affected by the experimental treatment. Different gas tensions are known to alter the expression levels of many genes, including several standard housekeeping genes, such as *GAPDH*, which are frequently used as internal reference genes in real-time RT PCR[122]. In order to investigate if the different gas tensions affected the *GAPDH* levels in the cells, the amounts of *GAPDH* from cells expanded in the different gas tensions were determined by real-time RT PCR. The relative amounts are presented using the $2^{-\Delta C't}$ method in figure 3-6.

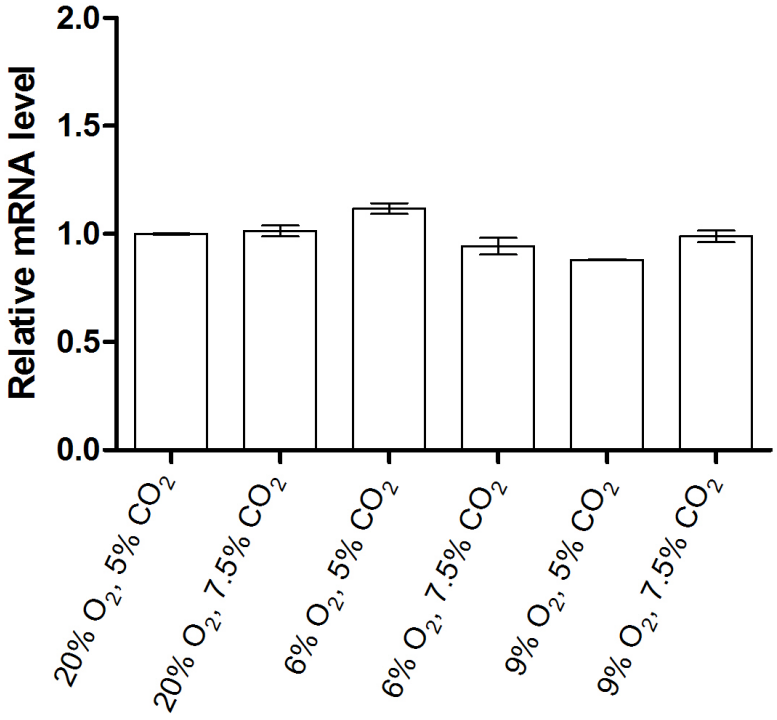

Figure 3-6. Validation of *GAPDH* as internal control. mRNA levels were scaled according to "20% O_2, 5% CO_2". This value was set to 1.Data are displayed as mean ± SD (n = 3). RNA input corresponding to 6 ng/replicate was used for external normalization. A two sample t-Test was used to test for significant changes in mRNA levels. $P \leq 0.05$ was considered significant.

There was no significant relationship between the gas tensions and the expression of *GAPDH*, indicating that the *GAPDH* levels in the cells were not affected by exposure to different gas tensions, and that the *GAPDH* expression level in the cells can be used as an internal reference for normalization of target genes measured by real-time RT PCR experiments.

3.4.4 Amplification efficiency of gene expression assays

Valid use of the $2^{-\Delta\Delta Ct}$ calculation requires that the PCR efficiencies of the target and reference amplicons are approximately equal[120]. To determine if the amplification efficiency of the *OCT-4*, *KLF4*, *C-MYC*, *NANOG*, and *SOX2* assays were similar to the *GAPDH* assay, a 3-fold dilution series of ECC derived RNA was made, and each of the five targets were amplified simultaneously with *GAPDH*. The ΔC_T value was calculated for every dilution, and a plot of log RNA input versus ΔC_T was produced (figure 3-7).

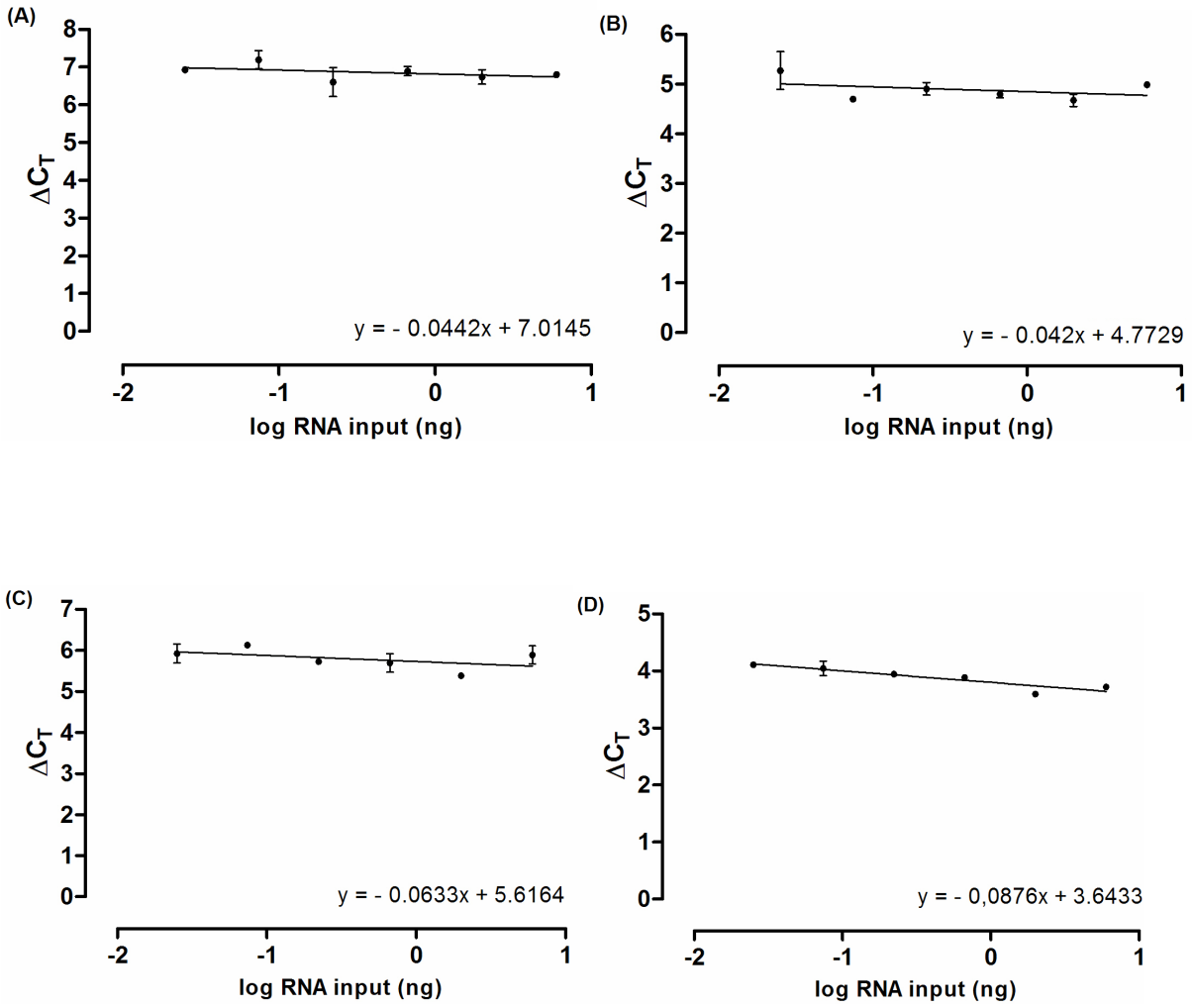

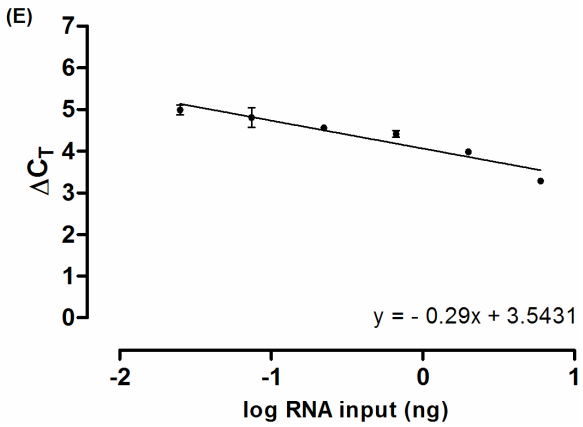

Figure 3-7. Relative efficiency plots of (A) *OCT-4*, (B) *KLF4*, (C) *C-MYC*, (D) *NANOG* and (E) *SOX2*. cDNA was synthesized from different amounts of RNA. RNA amount ranged from 0,025 ng RNA to 6 ng RNA. The amplification efficiency was examined using real-time RT PCR. Data are displayed as mean ± SD (n = 3)

The slope of the curves between *GAPDH* and *OCT-4*, *GAPDH* and *NANOG*, *GAPDH* and *KLF4*, and *GAPDH* and *C-MYC* was between 0.1 and -0.1. This result shows that the PCR efficiency of these assays was similar, and that these assays could be used in real-time RT PCR. The slope of the curve between *GAPDH* and *SOX2* was -0.29, demonstrating that the amplification efficiency of the two was not equal. Therefore, the *SOX2* assay was excluded from the experiment.

3.4.5 Expression of markers associated with primitive stem cell state

In order to assess whether the gas tension used for hBM-MSC culture affected expression of primitive stem cell markers, real-time RT PCR analyses were performed on cells at passage 2. The relative amount of *OCT-4*, *KLF4*, *C-MYC* and *NANOG* mRNA is presented using the $2^{-\Delta\Delta Ct}$ method in figure 3-8.

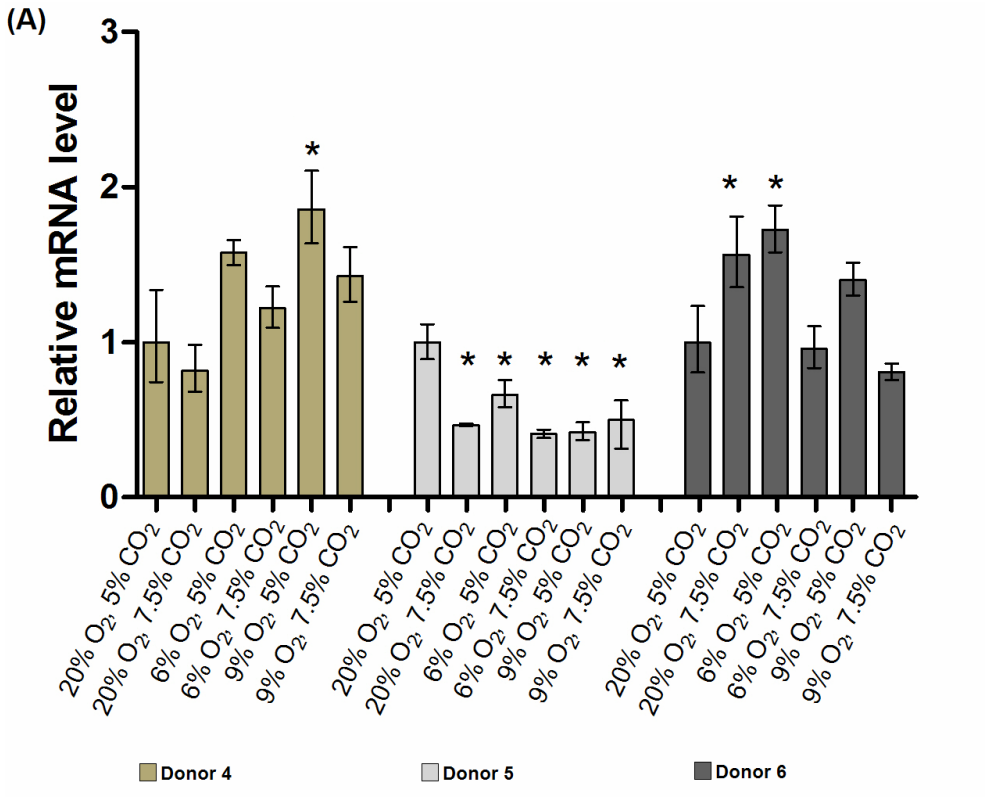
(A)
Relative mRNA level
0
1
2
3
20% O2, 5% CO2
20% O2, 7.5% CO2
6% O2, 5% CO2
6% O2, 7.5% CO2
9% O2, 5% CO2
9% O2, 7.5% CO2
Donor 4
Donor 5
Donor 6

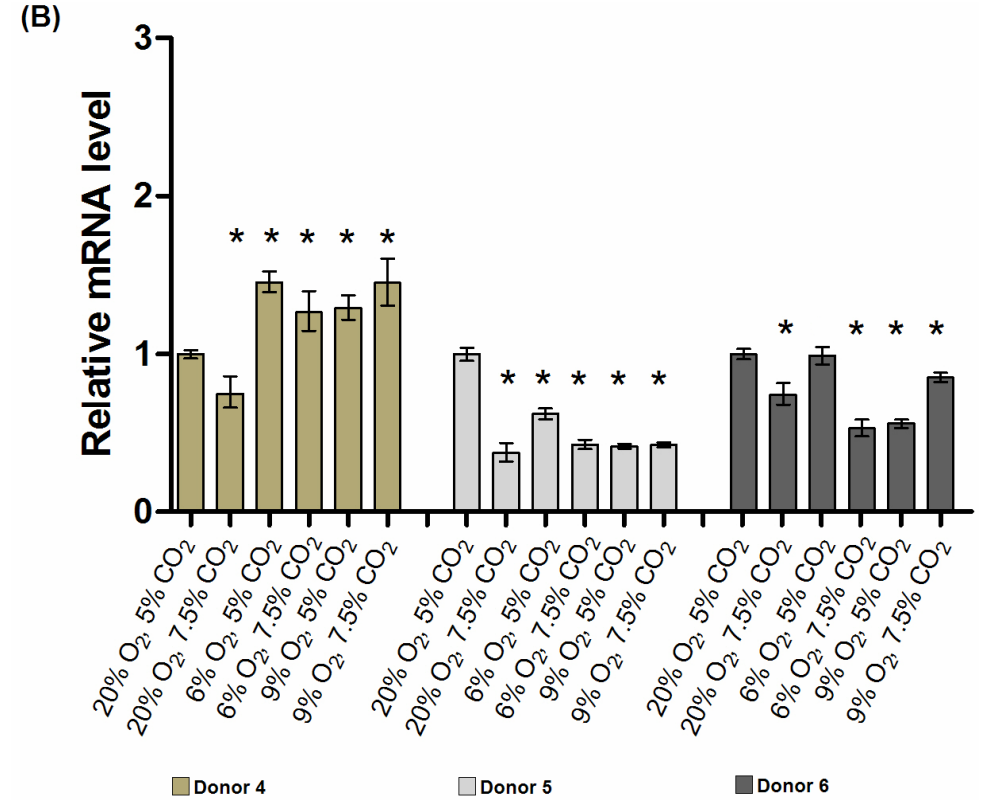
(B)
Relative mRNA level
0
1
2
3
20% O2, 5% CO2
20% O2, 7.5% CO2
6% O2, 5% CO2
6% O2, 7.5% CO2
9% O2, 5% CO2
9% O2, 7.5% CO2
Donor 4
Donor 5
Donor 6

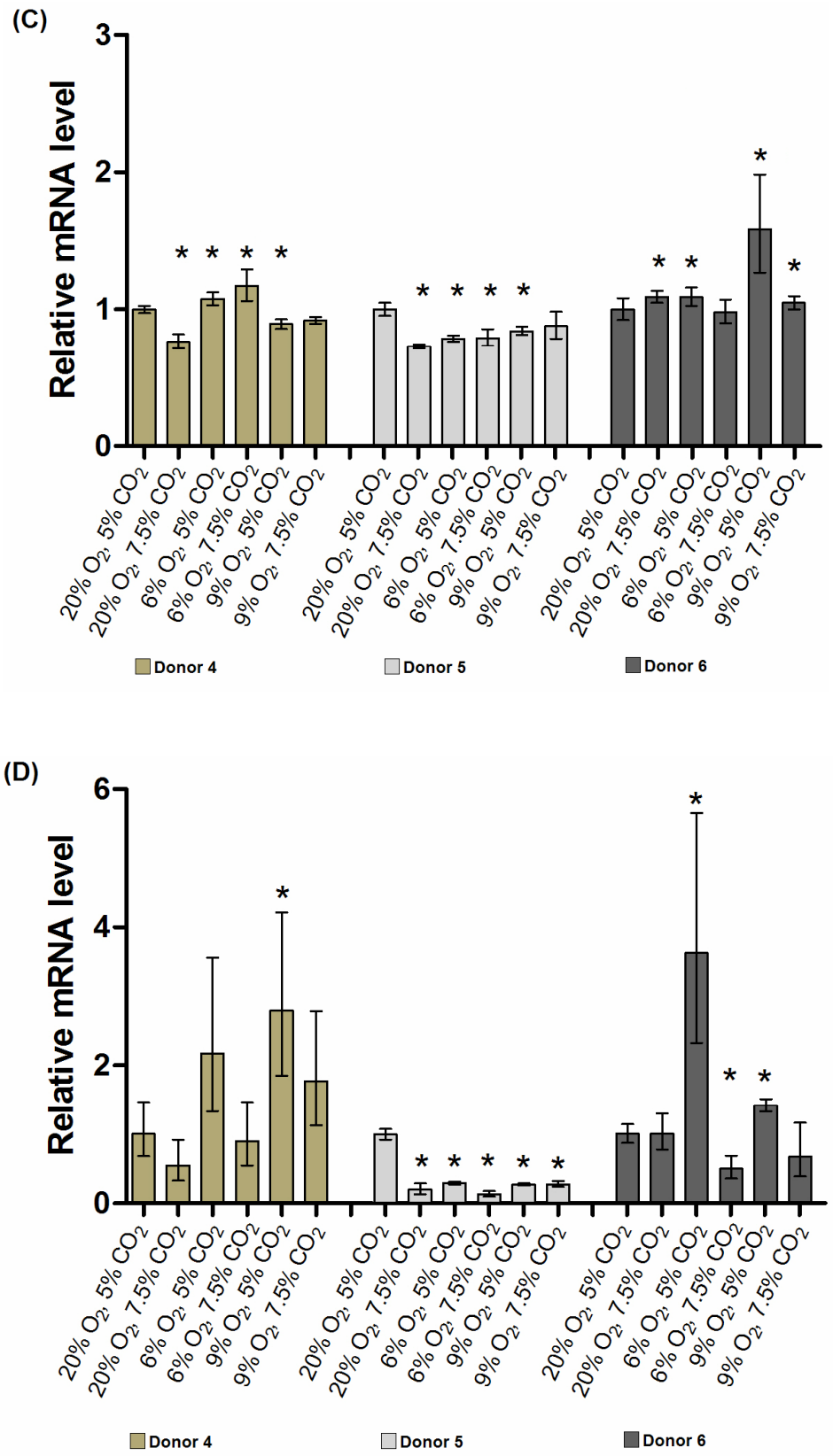

Figure 3-8. Relative expression was determined using real-time RT PCR. (A) Relative expression of *OCT-4*. (B) Relative expression of *KLF4*. (C) Relative expression of *C-MYC*. (D) Relative expression of *NANOG*. mRNA levels were scaled according to "20% O_2, 5% CO_2". This value was set to 1 (calibrator). Data are displayed as mean ± SD (n = 3). A two sample t-Test was used to test for significant changes in mRNA levels. Bonferroni corrections were applied to all experiments and $P \leq 0.05$ was considered significant. * = $P \leq 0.05$.

There was very little change in mRNA levels when scaled according to "20% O_2, 5% CO_2" (calibrator). However, some of the expression levels were statistically significant:

OCT-4

In donor 4 only one gas tension resulted in significant change in mRNA levels; hBM-MSC grown in "9% O_2, 5% CO_2" showed an increase in *OCT-4* expression. hBM-MSC from donor 5 had lower *OCT-4* mRNA levels in all gas tensions compared to the calibrator. In donor 6 up-regulation of *OCT-4* was found in hBM-MSC expanded in "20% O_2, 7.5% CO_2" and "6% O_2, 5% CO_2".

KLF4

hBM-MSC from donor 4 showed down-regulation of *KLF4* when expanded in "20% O_2, 7.5% CO_2" and up-regulation when expanded in the other gas tensions. In donor 5 the calibrator had the highest level of *KLF4* mRNA. hBM-MSC from donor 6 showed the same tendency as donor 5, except that "6% O_2, 5% CO_2" was not significantly different from the calibrator.

C-MYC

The *C-MYC* mRNA level in hBM-MSC from donor 4, expanded in "20% O_2, 7.5% CO_2" and "9% O_2, 5% CO_2" was reduced, while it was increased in "6% O_2, 5% CO_2" and "6% O_2, 7.5% CO_2". In donor 5, all gas tensions resulted in downregulation, except for "9% O_2, 7.5% CO_2" which was not statistically different from the calibrator. hBM-MSC in all gas tensions, except for "6% O_2, 7.5% CO_2", had higher expression of *C-MYC* relative to the calibrator in donor 6.

NANOG

The *NANOG* expression level in cells from donor 4 expanded in "9% O_2, 5% CO_2" was significantly increased, while the expression levels in cells grown at other gas tensions were similar to the calibrator. The calibrator had the highest expression of *NANOG* in donor 5. In donor 6, hBM-MSC expanded in "6% O_2, 5% CO_2" and "9% O_2, 5% CO_2" had elevated amounts of *NANOG*, while hBM-MSC in "6% O_2, 7.5% CO_2" had lower amounts.

Only down-regulation of *KLF4* in hBM-MSC grown in "20% O_2, 7.5% CO_2" were observed in cells from all three donors. Otherwise, there was no clear relationship between changed gene expression and gas tensions when comparing the three donors. All the statistically significant changes in gene expression levels detected in cells from donor 5 were reduced, while donor 4 and 6 had both reduced and increased expression levels compared to the calibrator.

3.5 Microarray

3.5.1 RNA integrity

Before analysis, using the Illumina bead system, the integrity of the RNA samples was checked before and after amplification of the RNA. The gel like image in figure 3-9 showed no RNA degradation before amplification.

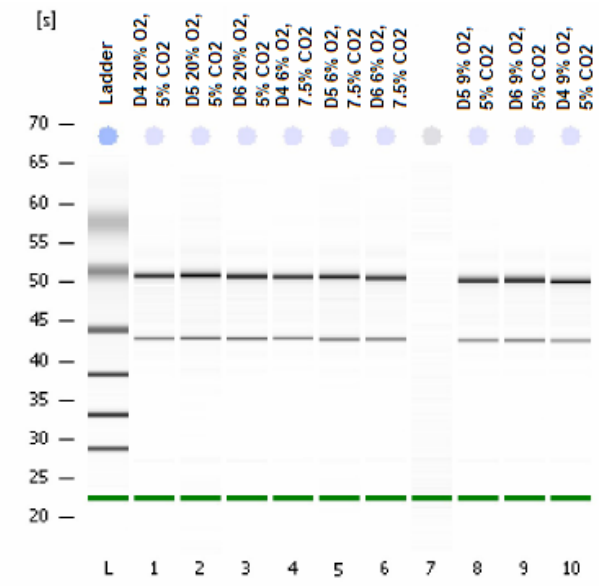

Figure 3-9. No RNA degradation could be observed in any of the samples before amplification of the RNA. Degradation would be reflected by smearing of the bands. D4 = Donor 4, D5 = Donor 5, D6 = Donor 6.

All samples had a RIN value of 10 (data not shown), which indicate intact RNA. Further, the amplified biotin labeled mRNA was not degraded (data not shown).

3.5.2 Clustering and pairwise comparisons

Service XS in Leiden performed chip quality analysis. All chips were of high quality (data not shown). However, hierarchical clustering (condition three) in Genespring was applied in order to see if there were any outliers among the samples. The condition three grouped the samples from the same donor into separate sub clusters, except for "Donor 5, 6% O_2, 7.5% CO_2", which had its own branch (figure 3-10).

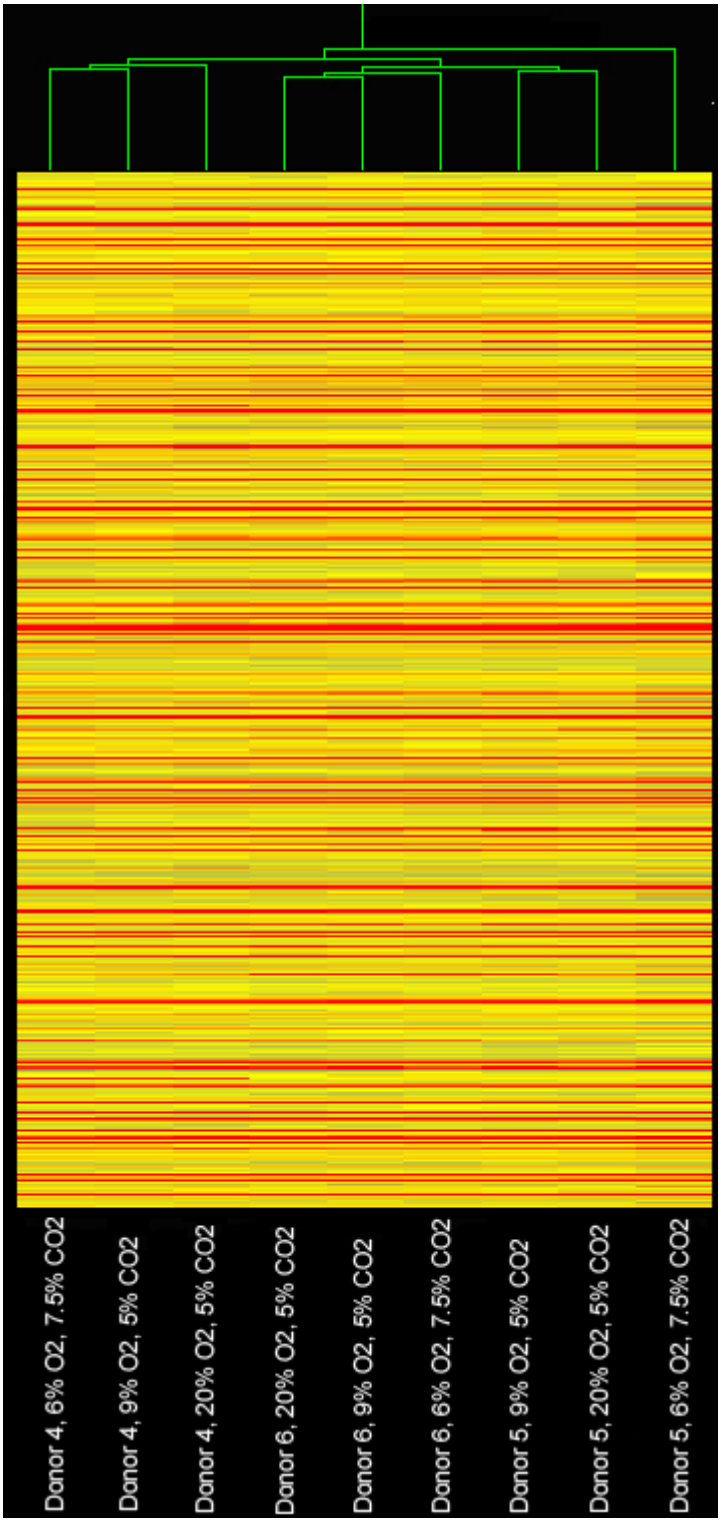

Figure 3-10. Samples were grouped together based on similar expression profiles. Each gene has been assigned a color based on the signal intensity. Yellow = normal expression, red = high expression, blue = low expression.

Generally, in this kind of experiments, samples that do not belong in any subcluster are potential outliers. In the condition three in figure 3-10, all pair of clusters had a correlation higher than 94% (including the correlation between "Donor 5, 6% O_2, 7.5% CO_2" and the rest of the samples), indicating no significant technical variation between the samples . Therefore,

no samples were removed from the experiment. In order to obtain a rough overview over the differently expressed genes, the different gas tensions were compared using scatterplots with 2-fold as cut-off value. A scatterplot comparing "20% O_2, 5% CO_2" with "6% O_2, 7.5% CO_2" is shown as an example in figure 3-11.

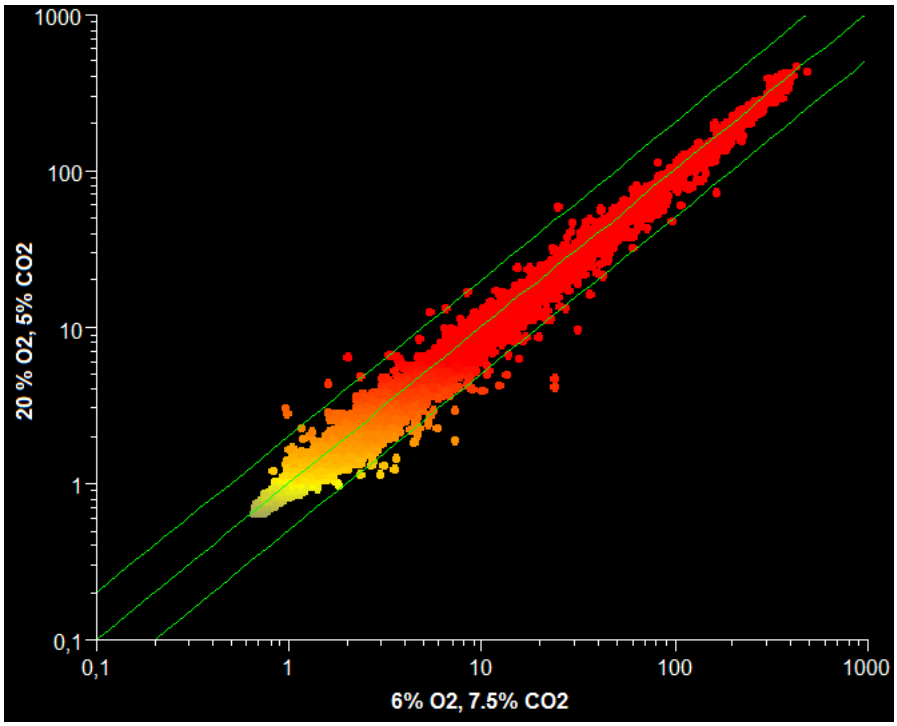

Figure 3-11.
This scatterplot shows a pairwise comparison between "20% O_2, 5% CO_2" and "6% O_2, 7.5% CO_2. The X and Y axes represent the expression levels in the two samples. For each gene on the beadchip, a single dot is placed at the intersection of these two values. All 46718 probes are represented in this plot. The two outer lines indicate a 2-fold difference, whereas the central line represents equality.

Out of the 46718 genes (probes) represented on the beadchip, 44 genes were differently expressed (>2-fold) between "20% O_2, 5% CO_2" and "6% O_2, 7.5% CO_2". For the comparisons between "20% O_2, 5% CO_2" and "9% O_2, 5% CO_2", and "6% O_2, 7.5% CO_2" and "9% O_2, 5% CO_2", 1 and 42 genes, respectively, were found to be differently expressed (>2-fold). In summary, these results show that few genes were differently expressed between hBM-MSC expanded in the different gas tensions.

3.5.3 Data analysis

In order to exclude data that are unlikely to be of biological interest, a quality control on the genes was applied. First, genes that showed large variability in gene expression were removed. Subsequently, genes with less than 1.5-fold change difference across the experiment

were excluded. The quality control reduced the number of genes from 46718 genes to 492 genes. This gene list was analyzed by one-way ANOVA, with 0.05 as false discovery rate. First, multiple testing correction was omitted. This resulted in 58 genes that were found to be differently expressed between the different gas tensions. Subsequently, pairwise comparisons between the different gas tensions were performed using volcano plots. A volcano plot comparing "20% O_2, 5% CO_2" with "6% O_2, 7.5% CO_2" is shown in figure 3-12.

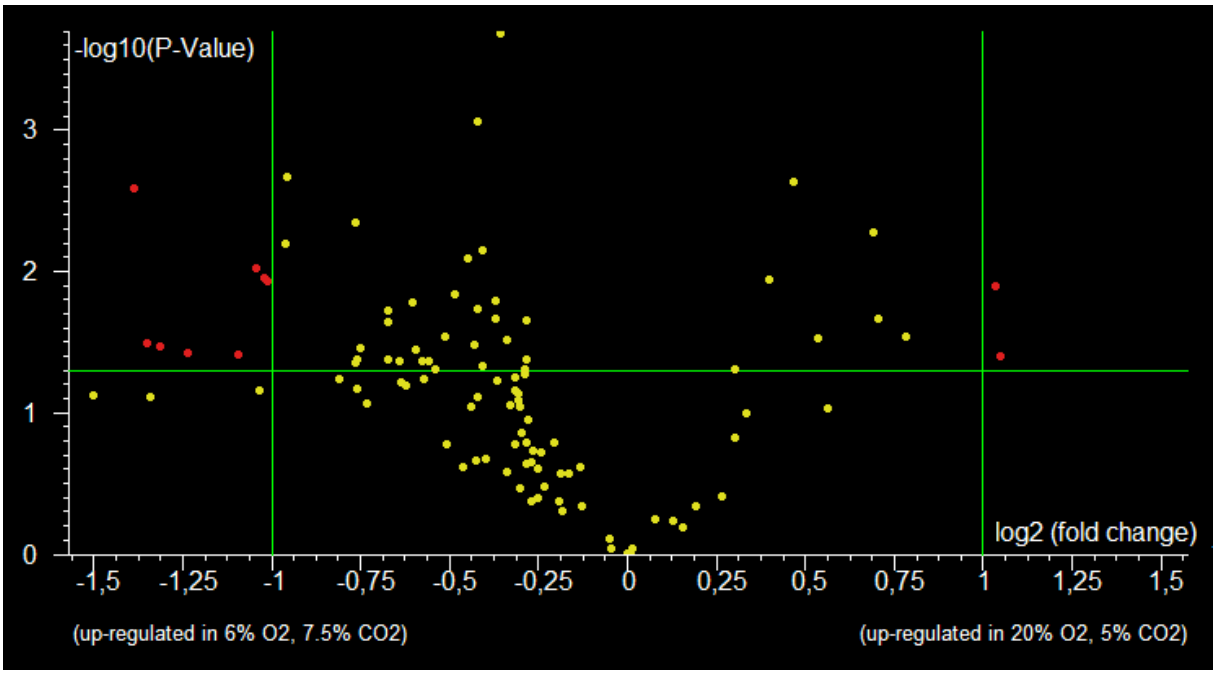

Figure 3-12. In this volcano plot, the size of the fold change between "20% O_2, 5% CO_2" and "6% O_2, 7.5% CO_2", is compared to the statistical significance level. The horizontal axis is the fold change between the two groups (on a log scale, so that up- and down-regulation appear symmetric). The vertical axis represents the p-value for a t-test of differences between samples. Each spot represent one gene. Genes with negative values on the x-axis represent genes that are up-regulated in "6% O_2, 7.5% CO_2" compared to "20% O_2, 5% CO_2". Genes with positive values on the x-axis represent genes that are up-regulated in "20% O_2, 5% CO_2" compared to "6% O_2, 7.5% CO_2". Equality is represented by 0. The two green vertical lines represent a 2-fold cut-off, and the green horizontal line represents a P-value of 0.05. The red spots represent genes that passed the restrictions.

In figure 3-11, eight genes were up-regulated in "6% O_2, 7.5% CO_2", while 2 genes were up-regulated in "20% O_2, 5% CO_2". Volcano plots were made for all comparisons. The genes that passed the volcano plot restrictions are presented in table 3-2, 3-3, 3-4 and 3-5.

Table 3-2. Genes up-regulated in "20% O_2, 5% CO_2" compared to "6% O_2, 7.5% CO_2".

Gene Name	GenBank accession no.	Fold change
Slit homolog 3 (Drosophila) (SLIT3)	NM_003062	2,067
Growth differentiation factor 5 (cartilage-derived morphogenetic protein-1) (GDF5)	NM_000557	2,051

Table 3-3. Genes up-regulated in "20% O_2, 5% CO_2" compared to "9% O_2, 5% CO_2".

Gene Name	GenBank accession no.	Fold change
Caldesmon 1 (CALD1)	NM_033138	2,035

Table 3-4. Genes up-regulated in "6% O_2, 7.5% CO_2" compared to "20% O_2, 5% CO_2".

Gene Name	GenBank accession no.	Fold change
Prostaglandin E synthase (PTGES)	NM_004878	2,617
Protein tyrosine phosphatase, receptor type, B (PTPRB)	NM_002837	2,544
Serpin peptidase inhibitor, clade G (C1 inhibitor), member 1 (SERPING1)	NM_000062	2,481
Zinc finger protein 185 (LIM domain) (ZNF185)	NM_007150	2,353
Insulin-like growth factor binding protein 3 (IGFBP3)	NM_001013398	2,137
Amyloid beta (A4) precursor protein-binding, family B (APBB1IP)	NM_019043	2,062
Sperm associated antigen 4 (SPAG4)	NM_003116	2,029
6-phosphofructo-2-kinase/fructose-2,6-biphosphatase 4 (PFKFB4)	NM_004567	2,016

Table 3-5. Genes up-regulated in "6% O_2, 7.5% CO_2" compared to "9% O_2, 5% CO_2".

Gene Name	GenBank accession no.	Fold change
Insulin-like growth factor binding protein 3 (IGFBP3)	NM_001013398	3,128
Prostaglandin E synthase (PTGES)	NM_004878	2,597
Serpin peptidase inhibitor, clade G (C1 inhibitor), member 1 (SERPING1)	NM_000062	2,516
Fibronectin type III domain containing 1 (FNDC1)	NM_032532	2,433
Protein tyrosine phosphatase, receptor type, B (PTPRB)	NM_002837	2,167
Periostin, osteoblast specific factor (POSTN)	NM_006475	2,145

No genes were found to be up-regulated in "9% O_2, 5% CO_2" compared to the two other gas tensions.

However, when omitting the multiple testing correction in the one-way ANOVA analysis, 25 of the 58 genes were expected to pass by chance (false positives). Almost half of the genes (42.4%) that passed the one-way ANOVA analysis can therefore be expected to be false positives. Thus, the gene lists in table 3-2, 3-3, 3-4, and 3-5 most likely contain many false positives. To reduce the number of false positives, the Benjamini and Hochberg multiple testing correction was applied in the one-way ANOVA. This restriction resulted in no significant change in gene expression between the different gas tensions.

4. Discussion

Standard incubator gas tensions corresponding to 20% O_2, and 5% CO_2 are routinely used for *in vitro* expansion of hBM-MSC, and it is being overlooked that such conditions do not correspond to the physiological gas tensions found in the bone marrow microenvironment. Therefore, the role of gas tensions in the expansion of hBM-MSC is not understood. As gas tension is an important component of the hBM-MSC niche, it may take part in the regulation of self-renewal and differentiation of hBM-MSC. In order to investigate the *in vitro* effects of different incubator gas tensions, hBM-MSC were cultured in six different gas tensions. Growth curves were made to assess the proliferative capability of the cells, real-time RT PCR analysis and microarray analysis was used to assess differences in gene expression.

FBS is generally used as nutritional supplement for *in vitro* expansion of hBM-MSC. However, in this thesis, AS was used as nutritional supplement. In order to reduce monocyte contamination, monocytes are frequently depleted from the BM-MNC fraction before culturing the cells. Observations have indicated reduced monocyte contamination when culturing hBM-MSC in AS (non-published data from Dr. Brinchmann's laboratory). Therefore, this study also aimed at examining if depletion of monocytes was necessary when using AS as nutritional supplement.

4.1 Choice of serum supplement

Serum is the clear liquid part of blood that remains after blood cells and clotting factors have been removed. The exact composition of serum is unknown, but it supplies the culture medium with essential cytokines, growth factors, antioxidants, fatty acids, hormones, and proteins that cells require during culture. *In vitro* hBM-MSC are expanded in culture medium containing 10% to 20 % serum, and until recently, FBS was the only serum choice. If hBM-MSC is to be used in cellular therapy, all animal-derived products should ideally be excluded because of possible contamination by prions, viruses or zoonoses infections[127]. Other problems concerning the use of FBS are immune reactions to fractions of bovine proteins, which may lead to antibody formation[128] and rejection of the transplanted cells. The use of serum supplements other than FBS is therefore desirable. Recently, AS and allogeneic human serum (alloHS) were examined to see if they could replace FBS for *in vitro* expansion of hBM-MSC. AS was shown to be as good as, or better than FBS, but the use of alloHS

resulted in growth arrest and cell death[24]. The use of AS could eliminate, or reduce the risk of contamination that follows the use of FBS. Hence, it may be the preferable choice of serum supplement for *in vitro* expansion of hBM-MSC for cellular therapy. Based on this, it was decided to use AS as serum supplement in this thesis. One potential limitation is the amount of AS needed to expand hBM-MSC on a clinical scale. AS is prepared from venous blood, and the maximum amount of venous blood that can be drained is 450 ml, which yields approximately 200 ml of AS. This amount is sufficient for expansion of hBM-MSC, derived from 60-80 ml bone marrow aspirate, to a total number between 50-80 millions. However, the total number of hBM-MSC will depend on the isolation procedure, culture method, amount of bone marrow aspirate, and the proliferation capability of the cells.

4.2 Cells

Established cell lines are often used for *in vitro* experiments, and since these cells often have been expanded in culture for a long time, they have to some extent adapted to life in culture. One the other hand, cells that are freshly isolated from the body are certainly not adapted to the same *in vitro* conditions. These cells may display characteristics that more resemble their *in vivo* properties, but at the same time they do not exhibit their true *in vivo* properties. In addition, donor specific differences are expected to be more distinct between freshly isolated cells compared to that of established cell lines. Ideally, if hBM-MSC are to be used in cell therapy, the patients own cells should be used. Therefore, freshly isolated hBM-MSC from the bone marrow were used in this thesis.

4.3 Monocyte depletion

Isolation of hBM-MSC is based on their ability to adhere to the culture substrate. However, this method often results in monocyte contamination. When expanding hBM-MSC in medium supplemented with FBS, depletion of monocytes seems to be necessary. Otherwise the culture substrate is largely occupied by contaminating monocytes. Previous observations indicate that monocyte contamination is significantly reduced when AS is used as serum supplement (non published data from Dr. Brinchmann's laboratory). Therefore, it was decided to test if depletion of monocytes were necessary when culturing hBM-MSC in AS. Monocytes can be depleted from the BM-MNC fration based on their expression of the CD14 molecule (section 2.4.2). According to observations in the light microscope, monocytes were not a significant

source of contamination in the cultures used in this study, and no distinct monocyte contamination was observed after the first passaging of the cells. This experiment indicate that monocyte depletion is unnecessary when expanding the cells in culture medium supplemented with AS. The factors responsible for this difference are unknown and remain to be identified. Another interesting observation was that depletion of monocytes resulted in poor yield of hBM-MSC colonies. What caused this difference in colony formation is unknown. A possible explanation may be unspecific binding of the CD14 antibodies during the cell separation procedure. As the aim of this experiment only was to test the necessity of depleting $CD14^+$ monocytes, no further investigation was pursued to identify the factors responsible for these differences.

4.4 Morphology

As observed in the light microscope, most hBM-MSC were thin and spindle shaped. However, a small portion of the cells were wide with a more flattened cytoplasmic volume. Under current *in vitro* culture condition, hBM-MSC can be expanded for 30-40 population doublings before they enter replicative senescence, which is characterized by growth arrest, and eventually cell death[129]. During cell division, the DNA polymerase is not able to replicate the end of the telomeres (the tip of linear chromosomes)[130, 131]. Hence, for every cell division the chromosomes become shorter. When the telomeres reach a critical length, the cells enter replicative senescence. Thus, there is a limit for how many cell divisions the hBM-MSC can go through. In the case of hBM-MSC, they become wide with a flattened cytoplasm when entering replicative senescence. Hence, the large, and wide hBM-MSC observed in the cultures had most likely gone through several cell divisions before they were isolated from the bone marrow. Therefore, it is likely that these cells were close to, or had entered replicative senescence.

4.5 Cell counts

In order to assess the proliferative capability of the cells, growth curves were made for all gas tensions. According to the growth curves, there were no consistent differences in cell counts between hBM-MSC expanded in 20%, 6% and 9% O_2 with both 5% and 7.5% CO_2 (figure 3-3). The small differences shown in figure 3-3 can be expected due to uncertainty in the counting procedure. Cell counts from donor 5 and 6 showed the same pattern as donor 4.

Hence, in the culture system used in this thesis, O_2 and CO_2 tension did not seem to affect the proliferation capability of polyclonal hBM-MSC.

4.6 RNA quality

mRNA is the starting material for real-time RT PCR and microarray analysis. The mRNA is always reverse transcribed into cDNA that can be used further in real-time RT PCR and microarray. To be of relevance, the amount of cDNA generated by the RT has to be proportional to the relative amount of its RNA template[121]. Thus, a prerequisite is that the mRNA is intact. Otherwise the RT reactions would yield varying amounts of cDNA. However, RNA is labile and susceptible to degradation. Therefore, it is always recommended to validate the RNA integrity before starting the RT reaction. Because real-time RT-PCR and microarray analysis was performed in two different laboratories in this thesis, RNA integrity was validated by two independent methods. The first method was based on separation of the RNA on an agarose gel. The second method was validation by the Agilent Bioanalyzer system. Both methods demonstrated high RNA integrity (figure 3-4 and 3-9), ensuring a good starting point for gene expression analysis.

4.7 Real-time RT PCR

4.7.1 Choice of targets and optimalisation

Verfaillie *et al.* induced expression of *OCT-4* by culturing MAPC clones in 5% O_2[116]. *OCT-4* is one of the major genes that are known to regulate self-renewal and differentiation of ESC. It was therefore interesting to examine if *OCT-4* mRNA levels changed during expansion of polyclonal hBM-MSC in different O_2 levels. Therefore, *OCT-4* was chosen as target for real-time RT PCR. Other genes associated with pluripotent stem cells were also investigated. *NANOG* is a transcription factor that is well known to regulate self-renewal and differentiation in ESC.[132, 10]. Thus, *NANOG* mRNA levels were also subjected to real-time RT PCR. Takahashi *et.al* induced pluripotent stem cells from mouse embryonic, and adult fibroblast by introducing *OCT-4*, *SOX2*, *KLF4* and *C-MYC* into the cells. All four genes was required to maintain the pluripotent properties of the cells[13]. Therefore *SOX2*, *KLF4*, and *C-MYC* mRNA levels were also used as targets in the real-time RT PCR. However, before quantifying the relative changes in mRNA levels of the selected genes, certain assumptions, and the testing of these assumptions were performed to properly analyze the data. In

summary, the important steps in the design of a real-time RT PCR experiment is to[121, 120]: (i) find proper amount of RNA input that will be efficiently reverse transcribed to cDNA, (ii) select an internal reference, and (iii) validate the internal reference to determine that it is not affected by experimental treatment. The last step is to determine the amplification efficiencies of the target and internal reference to ensure that the efficiency amplicons are similar.

Amplification of cDNA derived from different amounts of RNA was performed to assess the efficiency of the RT reaction (section 2.8.2). As demonstrated by the linear curve in figure 3-5, cDNA amounts produced were proportional with the amount of RNA input for all dilutions. Therefore, all RNA amounts were suitable. In order to determine if the internal reference (*GAPDH*) was affected by the different gas tensions, cDNA derived from hBM-MSC expanded in the different gas tensions were amplified by real-time RT PCR (section 2.8.3). In this experiment only one target was amplified. Therefore, an external normalisation had to be used[120]. A fixed amount of RNA (corresponding to 6 ng RNA/replicate) was used as the external normalisation. There was no relationship between the gas tensions and the expression of *GAPDH*, as shown in figure 3-6. Therefore, *GAPDH* was a suitable internal control for this gene expression experiment. Furthermore, the amplification efficiency of the targets and the internal reference was assessed by looking at how ΔC_T varied with template dilution (section 2.8.4). The *OCT-4*, *NANOG*, *KLF4* and *C-MYC* assays had amplification efficiencies similar to that of *GAPDH*, and were therefore suitable for relative quantification using real-time RT PCR. The curve obtained after comparing the *GAPDH* and *SOX2* assays, had a slope of -0.29, showing that the amplification efficiency of the two was not similar (figure 3-7). Thus, the *SOX2* assay was not suitable for RQ using real-time RT PCR, and was therefore excluded from the experiment. If *SOX2* had been very important for us, the analysis could be performed via the absolute quantification method using standard curves. Alternatively, new primers could be used.

4.7.2 Relative quantification

For the relative quantification analysis, all mRNA levels were scaled according to standard incubator gas tension (20% O_2, 5% CO_2). Only small fold changes were detected, below two-fold for most comparisons. A two-fold change can be at the limit of detection of real-time RT PCR[133]. Small fluctuations in the starting material will lead to relatively high fluctuations in the amount of product, which is expressed in C_T values (a C_T difference of one represents a

two-fold difference in starting material). Therefore, a two-fold difference in mRNA levels may be due to methodological variability. However, some of the fold changes were found to be statistically significant, but there was no consistent pattern regarding expression of *OCT-4*, *NANOG*, *KLF4*, and *C-MYC* in the different gas tensions (figure 3-8). Only reduced *KLF4* mRNA levels, in 20% O_2 and 7.5% CO_2, was shared between the three donors. Beyond that, the rest of the results were inconsistent. For example, in hBM-MSC from donor 4, there was a higher expression of *OCT-4* in 9% O_2 and 7.5% CO_2 compared to the standard incubator gas tension. In the same comparison for donor 5, *OCT-4* mRNA levels were found to be reduced. On the other hand, in donor 6, *OCT-4* mRNA levels were not significantly changed. Due to the small fold changes, and the lack of consistent pattern in gene expression, gas tension did not seem to affect expression of markers associated with pluripotent stem cells. In addition, the fold changes that were found to be statistically significant were based on three technical replicates (replicates from same donor and same gas tension). Technical replicates reduce the effects of variation introduced by the technology used, but it does not reduce the effects of biological variation (donor specific differences). If the results from the three donors had been used as biological replicates (that is, replicates consist of samples from different donors, but from the same gas tension), the effects of biological variation would have been reduced. As a result, the fold change differences would most likely have been reduced and fewer measurements would have been significant.

4.8 Microarray

Due to economical issues, only "20% O_2, 5% CO_2", "6% O_2, 7.5% CO_2", and "9% O_2, 5% CO_2" were analyzed by microarray. After discussing the experimental design with the Microarray core facility at Rikshospitalet-Radiumhospitalet, it was decided to use samples from the same gas tension (different donors) as biological replicates. Service XS in Leiden, the Netherlands, performed beadchip quality analysis, and confirmed that the beadchips was of high quality. After receiving the data files, they were imported into Genespring GX 7.3.1 for analysis (section 2.9.2). As a quality control on the samples, a hierarchical clustering (condition three) was performed. The condition three clustered the samples into 3 subclusters, and one branch. The subclusters consisted of samples derived from the same donor. For donor 5, two of the samples were grouped together, while "Donor 5, 6% O_2, 7.5% CO_2" had its own branch (figure 3-10). Because "Donor 5, 6% O_2, 7.5% CO_2" was placed alone in the condition three, it was a potential outlier. However, the correlation between "Donor 5, 6% O_2, 7.5%

CO_2" and the rest of the samples was higher than 94% (this was true for all pair of clusters). The correlation is related to the technical variation that can be introduced during the microarray procedure. A correlation higher than 90% is considered high, with little technical variation between samples, while 70-75% correlation is the absolute minimum criterion. Therefore, "Donor 5, 6% O_2, 7.5% CO_2" was not considered an outlier. Before starting the thoroughly analysis, the differences in gene expression were roughly assessed using pairwise comparisons (scatterplots) of the different gas tensions (figure 3-11). With a two-fold cut-off, 44 of the 46718 genes in the beadchip were differently expressed when comparing "20% O_2, 5% CO_2" and "6% O_2, 7.5% CO2". Comparison between "20% O_2, 5% CO_2" and "9% O_2, 5% CO2", showed only 1 gene with changed expression. The last comparison between "6% O_2, 7.5% CO2" and "9% O_2, 5% CO2" resulted in 42 differently expressed genes.

The beadchip that was used to obtain the data files contained probes for many genes that were either not expressed, expressed only in a few samples, or expressed at relatively constant levels. It is always a good strategy to remove these genes prior to performing other operations. Therefore, a quality control on the genes was performed. To do this, genes with high variability around the mean, and genes whose expression did not change more than 1.5-fold, between the different gas tensions, were removed from the data set. The resulting gene list was then reduced from 46718 genes to 492 genes. To obtain genes with statistical significance, a one-way ANOVA was applied on the 492 genes. Without multiple testing correction, 58 genes were found to be differently expressed between the different gas tensions. With a false discovery rate of 5%, 25 genes were expected to pass the one-way ANOVA restriction by chance (false positives). However, pairwise comparisons between the different gas tensions were performed using volcano plots (figure 3-12). Gene lists in table 3-2, 3-3, 3-4, and 3-5 show the genes that passed the volcano plot restrictions.

Although the gene lists obtained could contain false positives, it was still decided to determine the possible biological relevance of differential expression of these genes. For example, Growth differentiation factor 5 (GDF5), which was up-regulated in "20% O_2, 5% CO_2" compared to "6% O_2, 7.5% CO_2", is a member of the BMP family and the TGF-β superfamily[134]. The members of this family are regulators of cell growth and differentiation, and have been showed to regulate chondrogensis[79, 80, 135]. GDF5 is also involved in nervous system development, according to the gene ontology in Genespring (data not shown). Prostaglandin E synthase (PTGES), 6-phosphofructo-2kinase/fructose-2,6-bisphosphatase 4

(PFKFB4), and Insulin-like growth factor binding protein 3 (IGFBP3) were among the genes that were up-regulated in "6% O_2, 7.5% CO_2", when compared to "20% O_2, 5% CO_2". PTGES and PFKFB4 have been shown to be up-regulated in rBM-MSC when cultured in low O_2 tension (1%)[136]. PTGES is an enzyme which is induced by proinflammatory stimuli, and is down-regulated by anti-inflammatory glucocorticoids[137]. PFKFB4 is an activator of glycolysis, and are known to be induced by low O_2 tensions[138, 139]. According to gene ontology in Genespring, IGFBP3 are involved in skeletal muscle development (data not shown), and have also been shown to be up-regulated in low O_2 tensions (2% O_2)[140]. PTGES and IGFBP3 were also up-regulated in "6% O_2, 7.5% CO_2", when compared to "9% O_2, 5% CO_2". Although statistical considerations suggest that these genes may be falsely represented on the list of differentially expressed genes, the fact that they have been shown to be induced by low O_2 tensions in other datasets may indicate that the upregulation of these genes in "6% O_2, 7.5% CO_2" may actually be real. No genes were found up-regulated in "9% O_2, 5% CO_2" compared to the two other gas tensions. Although these findings were interesting, it is important to emphasize that almost half of the genes that passed the one-way ANOVA analysis were expected to pass by chance. On the other hand, it should not be completely ruled out that a few of the genes may be significant, but the results should be interpreted with great caution. Many researchers choose real-time RT PCR as a supporting technique to validate and better quantify the most interesting genes from their arrays. However, it was decided not to do this, because no genes were found differently expressed when applying multiple correction in the one-way ANOVA analysis (see below). In addition, the lower the fold change differences, the less correlation is seen between real-time RT PCR and microarray results, making the validation less reliable[141]. The low fold change differences in this experiment may be at the boundary where microarray and real-time RT PCR data begin to lose correlation.

To reduce the number of false positives, in order to obtain more reliable data, the one-way ANOVA analysis was repeated using multiple testing correction (Benjamini and Hochberg). This resulted in no differently expressed genes between the different gas tensions. Thus, the main conclusion of the microarray analysis is that gas tension did not affect the global gene expression of polyclonal hBM-MSC. It is worth mentioning that the data files also were analyzed in another analysis platform (Bioconductor) (by another independent investigator - Morten Mattingsdal from the Microarray core facility at Rikshospitalet-Radiumhospitalet). As in Genspring, no genes were found differently expressed when analyzing the data in

Bioconductor. This confirmed the results, and thereby strengthened the conclusion that gas tension did not affect the global gene expression in the cells. Microarray was performed on hBM-MSC expanded in three of the six different gas tensions. However, it is reasonable to assume that the results were representative for hBM-MSC expanded in all gas tensions.

Taking together the data from the growth curves, the real-time RT PCR, and the microarray analysis, all results indicate that the different incubator gas tension used in this thesis do not have an effect on the *in* vitro expansion of polyclonal hBM-MSC.

4.9 Considerations

Verfaillie *et al.* cultured rat MAPC at very low cell density (300 cell/cm^2), and in a serum concentration of 2%[116]. Maybe there would be a difference in gene expression if the same conditions had been used in this study. However, the effect of serum concentration of 2% needs to be examined with hBM-MSC, before such studies can be performed. In addition, if hBM-MSC are to be used in cell therapy, huge amounts of cells is required. By plating cells on densities corresponding to 300 cells/cm^2, the culture surface needed would be enormous. In the laboratory used during this thesis, it is practically impossible to expand the cells to quantities required for cell therapy, at such low cell densities. Thus, the culture system used in this thesis was the most suitable for this study.

Recently, several studies have investigated the effects of low O_2 tensions on MSC with contrasting results. For example, hBM-MSC expanded in 2% O_2, increased proliferation and expressed higher levels of *OCT-4*[142]. Another study where hBM-MSC were expanded in 1.5% O_2, also showed an increase in proliferation. In addition, 45 genes were reported to be up-regulated, and several of the genes were known to be regulated by O_2 tension[110]. rBM-MSC enhanced transcription of genes involved in cell proliferation and survival when cultured in 1% O_2[136]. Another study with rBM-MSC increased proliferation and enhanced osteoblast differentiation when grown in 5% O_2[112]. On the other hand, murine adipose derived MSC (mAT-MSC) showed enhanced proliferation, but reduced osteogenesis and chondrogenesis in 2% O_2[143]. Human adipose derived MSC (hAT-MSC) lowered proliferation and enhanced their chondrogenic differentiation in 5% O_2[144]. These conflicting data may be explained by different isolation methods, culture methods, type of culture (3D construct and monolayer), species differences, tissue of origin, and differences in O_2 tension. Therefore, it is also

difficult to compare these results with the results obtained in this thesis. However, in most of these studies, the cells were cultured in 2% O_2, or below. In such low O_2 levels, the cells may switch from aerobe to anaerobe metabolism. This would for certain alter their gene expression. Hypoxia-Inducible Factor 1α (Hif-1α) is a transcription factor that has been shown to be expressed under such conditions[145]. The stability and activation of Hif-1α is highly regulated by O_2 tension. The gene is constitutively expressed at the transcriptional level, but the protein is degraded when O_2 levels exceed 2%[145]. Hif-1α controls expression of many genes. Some of them are involved in cellular differentiation, such as erythropoietin (EPO), transferrin, transferrin receptor, vascular endothelial growth factor (VEGF), platelet-derived growth factor β (PDGF- β), and basic fibroblast growth factor (bFGF)[146-149]. In addition, Hif-activation results in increased expression of *OCT-4*[150]. Conversely, the differentiation gene PPAR-γ is down regulated as a result of Hif-activation[151]. In this thesis, hBM-MSC were not subjected for such low O_2 tensions, because these O_2 tensions are most likely below the physiological O_2 tension in the bone marrow. This may explain why there were no differences in cell counts and gene expression in the cell cultures used in this thesis. During cell culture, trypsin was used to lift the cells from the culture surface. Hence, the cells were exposed to the gas tensions in the trypsin solution for approximately seven minutes, before the RNA isolation procedure. It is possible that this also affected the gene expression, and reduced possible differences.

There is also a small possibility that some genes were regulated at the protein level. These genes would not be detected in this experiment, because the real-time RT PCR and microarray analysis quantified the mRNA levels in the cells. This is a major drawback with use of RNA analysis methods. The control of gene expression can occur at any step in the pathway from gene to functional protein[152]. Thus, gene expression may be regulated after synthesis of the mRNA molecules. For example, mRNA degradation, translation initiation, and protein processing and degradation are stages were cells can regulate their gene expression[152]. By using regulatory mechanisms that operate after transcription, cells can fine-tune gene expression in response to environmental changes without altering their transcription patterns. Therefore, real-time RT PCR and microarray analysis do not always reflect the real gene expression changes in cells. On the other hand, if a gene is found to be differently expressed by real-time RT PCR, or microarray, protein quantification methods can be a good strategy to validate that the gene is differently expressed at the protein level as well.

The previous studies, mentioned above, investigated the effects of low O_2 tension on MSC, and compared with cells cultured at the traditional 20% O_2 condition (hyperoxia)[110, 136, 142-144]. When hBM-MSC are expanded in hyperoxia, they are introduced to very high O_2 levels that they never have experienced before. Depending on the experimental settings, it may be relevant to study the effects of hyperoxia, instead of the effects of low O_2 tension. For example, do cells increase expression of *OCT-4* when cultured in O_2 tensions corresponding to normoxia, or is the expression reduced when the cells are introduced to hyperoxia? This may be a matter of terminology, but it is worth keeping in mind when performing experiments like this.

5. Conclusion

5.1 Depletion of CD14+ cells.

- Monocytes were not a significant source of contamination when hBM-MSC were cultured in AS. Therefore, depletion of $CD14^+$ cells seems to be unnecessary, prior to culture.
- Depletion of $CD14^+$ cells gave poor yield of hBM-MSC colonies

What caused these differences is not known and remains to be identified.

5.2 The in vitro effects of different incubator gas tensions on hBM-MSC.

- Incubator gas tension did not seem to have an effect on the proliferative capability of the cells, as there were no consistent differences in cell counts between hBM-MSC expanded in the different gas tensions.
- Results from real-time RT PCR analysis indicated that the expression of *OCT-4*, *NANOG*, *KLF4*, and *C-MYC* mRNA levels, were not affected by the different incubator gas tensions.
- The global gene expression of hBM-MSC was not significantly changed due to the different incubator gas tensions, as determined by microarray analysis.

References

1. Raff M. Adult stem cell plasticity: fact or artifact? Annu Rev Cell Dev Biol. 2003;19:1-22.
2. Moore KA, Lemischka IR. Stem cells and their niches. Science. 2006;311:1880-1885.
3. Thomson JA, Itskovitz-Eldor J, Shapiro SS, et al. Embryonic stem cell lines derived from human blastocysts. Science. 1998;282:1145-1147.
4. Meachem S, von Schonfeldt V, Schlatt S. Spermatogonia: stem cells with a great perspective. Reproduction. 2001;121:825-834.
5. Bongso A, Richards M. History and perspective of stem cell research. Best Pract Res Clin Obstet Gynaecol. 2004;18:827-842.
6. Rodda SJ, Kavanagh SJ, Rathjen J, et al. Embryonic stem cell differentiation and the analysis of mammalian development. Int J Dev Biol. 2002;46:449-458.
7. Beddington RS, Robertson EJ. Axis development and early asymmetry in mammals. Cell. 1999;96:195-209.
8. McKay R. Stem cells--hype and hope. Nature. 2000;406:361-364.
9. Niwa H, Miyazaki J, Smith AG. Quantitative expression of Oct-3/4 defines differentiation, dedifferentiation or self-renewal of ES cells. Nat Genet. 2000;24:372-376.
10. Yates A, Chambers I. The homeodomain protein Nanog and pluripotency in mouse embryonic stem cells. Biochem Soc Trans. 2005;33:1518-1521.
11. Avilion AA, Nicolis SK, Pevny LH, et al. Multipotent cell lineages in early mouse development depend on SOX2 function. Genes Dev. 2003;17:126-140.
12. Cartwright P, McLean C, Sheppard A, et al. LIF/STAT3 controls ES cell self-renewal and pluripotency by a Myc-dependent mechanism. Development. 2005;132:885-896.
13. Takahashi K, Yamanaka S. Induction of pluripotent stem cells from mouse embryonic and adult fibroblast cultures by defined factors. Cell. 2006;126:663-676.
14. Grove JE, Bruscia E, Krause DS. Plasticity of bone marrow-derived stem cells. Stem Cells. 2004;22:487-500.
15. Wagers AJ, Weissman IL. Plasticity of adult stem cells. Cell. 2004;116:639-648.
16. Serafini M, Verfaillie CM. Pluripotency in adult stem cells: state of the art. Semin Reprod Med. 2006;24:379-388.
17. Suda T, Arai F, Shimmura S. Regulation of stem cells in the niche. Cornea. 2005;24:S12-S17.
18. NIH. Stem cells: Scientific progress and future research directions: National Institute of Health, NIH; 2001.
19. Faulkner J, Keirstead HS. Human embryonic stem cell-derived oligodendrocyte progenitors for the treatment of spinal cord injury. Transpl Immunol. 2005;15:131-142.
20. Lea T. Immunologi og immunologiske teknikker: Fagbokforlaget; 2006: 243-250.
21. Horwitz EM, Prockop DJ, Fitzpatrick LA, et al. Transplantability and therapeutic effects of bone marrow-derived mesenchymal cells in children with osteogenesis imperfecta. Nat Med. 1999;5:309-313.
22. Horwitz EM, Gordon PL, Koo WK, et al. Isolated allogeneic bone marrow-derived mesenchymal cells engraft and stimulate growth in children with osteogenesis imperfecta: Implications for cell therapy of bone. Proc Natl Acad Sci U S A. 2002;99:8932-8937.

23. Francois S, Bensidhoum M, Mouiseddine M, et al. Local irradiation not only induces homing of human mesenchymal stem cells at exposed sites but promotes their widespread engraftment to multiple organs: a study of their quantitative distribution after irradiation damage. Stem Cells. 2006;24:1020-1029.
24. Shahdadfar A, Fronsdal K, Haug T, et al. In vitro expansion of human mesenchymal stem cells: choice of serum is a determinant of cell proliferation, differentiation, gene expression, and transcriptome stability. Stem Cells. Vol 23; 2005:1357-1366.
25. Friedenstein AJ, Chailakhjan RK, Lalykina KS. The development of fibroblast colonies in monolayer cultures of guinea-pig bone marrow and spleen cells. Cell Tissue Kinet. 1970;3:393-403.
26. Pittenger MF, Mackay AM, Beck SC, et al. Multilineage potential of adult human mesenchymal stem cells. Science. 1999;284:143-147.
27. Haynesworth SE, Goshima J, Goldberg VM, et al. Characterization of cells with osteogenic potential from human marrow. Bone. 1992;13:81-88.
28. Zuk PA, Zhu M, Mizuno H, et al. Multilineage cells from human adipose tissue: implications for cell-based therapies. Tissue Eng. 2001;7:211-228.
29. Boquest AC, Shahdadfar A, Brinchmann JE, et al. Isolation of stromal stem cells from human adipose tissue. Methods Mol Biol. 2006;325:35-46.
30. Bosch P, Musgrave DS, Lee JY, et al. Osteoprogenitor cells within skeletal muscle. J Orthop Res. 2000;18:933-944.
31. Song L, Young NJ, Webb NE, et al. Origin and characterization of multipotential mesenchymal stem cells derived from adult human trabecular bone. Stem Cells Dev. 2005;14:712-721.
32. Young HE, Steele TA, Bray RA, et al. Human reserve pluripotent mesenchymal stem cells are present in the connective tissues of skeletal muscle and dermis derived from fetal, adult, and geriatric donors. Anat Rec. 2001;264:51-62.
33. Zvaifler NJ, Marinova-Mutafchieva L, Adams G, et al. Mesenchymal precursor cells in the blood of normal individuals. Arthritis Res. 2000;2:477-488.
34. Eyckmans J, Luyten FP. Species specificity of ectopic bone formation using periosteum-derived mesenchymal progenitor cells. Tissue Eng. 2006;12:2203-2213.
35. Yamazaki H, Tsuneto M, Yoshino M, et al. Potential of dental mesenchymal cells in developing teeth. Stem Cells. 2007;25:78-87.
36. Shirasawa S, Sekiya I, Sakaguchi Y, et al. In vitro chondrogenesis of human synovium-derived mesenchymal stem cells: optimal condition and comparison with bone marrow-derived cells. J Cell Biochem. 2006;97:84-97.
37. Kaviani A, Perry TE, Dzakovic A, et al. The amniotic fluid as a source of cells for fetal tissue engineering. J Pediatr Surg. 2001;36:1662-1665.
38. Miao Z, Jin J, Chen L, et al. Isolation of mesenchymal stem cells from human placenta: comparison with human bone marrow mesenchymal stem cells. Cell Biol Int. 2006;30:681-687.
39. Bieback K, Kern S, Kluter H, et al. Critical parameters for the isolation of mesenchymal stem cells from umbilical cord blood. Stem Cells. 2004;22:625-634.
40. Colter DC, Class R, DiGirolamo CM, et al. Rapid expansion of recycling stem cells in cultures of plastic-adherent cells from human bone marrow. Proc Natl Acad Sci U S A. 2000;97:3213-3218.
41. Conget PA, Minguell JJ. Phenotypical and functional properties of human bone marrow mesenchymal progenitor cells. J Cell Physiol. 1999;181:67-73.
42. Dominici M, Le Blanc K, Mueller I, et al. Minimal criteria for defining multipotent mesenchymal stromal cells. The International Society for Cellular Therapy position statement. Cytotherapy. 2006;8:315-317.

43. Le Blanc K, Tammik C, Rosendahl K, et al. HLA expression and immunologic properties of differentiated and undifferentiated mesenchymal stem cells. Exp Hematol. 2003;31:890-896.
44. Tropel P, Noel D, Platet N, et al. Isolation and characterisation of mesenchymal stem cells from adult mouse bone marrow. Exp Cell Res. 2004;295:395-406.
45. Muraglia A, Cancedda R, Quarto R. Clonal mesenchymal progenitors from human bone marrow differentiate in vitro according to a hierarchical model. J Cell Sci. 2000;113 (Pt 7):1161-1166.
46. Awad HA, Boivin GP, Dressler MR, et al. Repair of patellar tendon injuries using a cell-collagen composite. J Orthop Res. 2003;21:420-431.
47. Pittenger MF, Martin BJ. Mesenchymal stem cells and their potential as cardiac therapeutics. Circ Res. 2004;95:9-20.
48. Kawada H, Fujita J, Kinjo K, et al. Nonhematopoietic mesenchymal stem cells can be mobilized and differentiate into cardiomyocytes after myocardial infarction. Blood. 2004;104:3581-3587.
49. Shiota M, Heike T, Haruyama M, et al. Isolation and characterization of bone marrow-derived mesenchymal progenitor cells with myogenic and neuronal properties. Exp Cell Res. 2007;313:1008-1023.
50. Woodbury D, Schwarz EJ, Prockop DJ, et al. Adult rat and human bone marrow stromal cells differentiate into neurons. J Neurosci Res. 2000;61:364-370.
51. Jiang Y, Jahagirdar BN, Reinhardt RL, et al. Pluripotency of mesenchymal stem cells derived from adult marrow. Nature. 2002;418:41-49.
52. Aggarwal S, Pittenger MF. Human mesenchymal stem cells modulate allogeneic immune cell responses. Blood. 2005;105:1815-1822.
53. Le Blanc K, Rasmusson I, Sundberg B, et al. Treatment of severe acute graft-versus-host disease with third party haploidentical mesenchymal stem cells. Lancet. 2004;363:1439-1441.
54. Krampera M, Glennie S, Dyson J, et al. Bone marrow mesenchymal stem cells inhibit the response of naive and memory antigen-specific T cells to their cognate peptide. Blood. 2003;101:3722-3729.
55. Di Nicola M, Carlo-Stella C, Magni M, et al. Human bone marrow stromal cells suppress T-lymphocyte proliferation induced by cellular or nonspecific mitogenic stimuli. Blood. 2002;99:3838-3843.
56. Ramalho-Santos M, Yoon S, Matsuzaki Y, et al. "Stemness": transcriptional profiling of embryonic and adult stem cells. Science. 2002;298:597-600.
57. Ivanova NB, Dimos JT, Schaniel C, et al. A stem cell molecular signature. Science. 2002;298:601-604.
58. Bruno L, Hoffmann R, McBlane F, et al. Molecular signatures of self-renewal, differentiation, and lineage choice in multipotential hemopoietic progenitor cells in vitro. Mol Cell Biol. 2004;24:741-756.
59. Abeyta MJ, Clark AT, Rodriguez RT, et al. Unique gene expression signatures of independently-derived human embryonic stem cell lines. Hum Mol Genet. 2004;13:601-608.
60. Brandenberger R, Wei H, Zhang S, et al. Transcriptome characterization elucidates signaling networks that control human ES cell growth and differentiation. Nat Biotechnol. 2004;22:707-716.
61. Wen T, Gu P, Minning TA, et al. Microarray analysis of neural stem cell differentiation in the striatum of the fetal rat. Cell Mol Neurobiol. 2002;22:407-416.

62. Song L, Webb NE, Song Y, et al. Identification and functional analysis of candidate genes regulating mesenchymal stem cell self-renewal and multipotency. Stem Cells. 2006;24:1707-1718.
63. Etheridge SL, Spencer GJ, Heath DJ, et al. Expression profiling and functional analysis of wnt signaling mechanisms in mesenchymal stem cells. Stem Cells. 2004;22:849-860.
64. Boland GM, Perkins G, Hall DJ, et al. Wnt 3a promotes proliferation and suppresses osteogenic differentiation of adult human mesenchymal stem cells. J Cell Biochem. 2004;93:1210-1230.
65. Kleber M, Sommer L. Wnt signaling and the regulation of stem cell function. Curr Opin Cell Biol. 2004;16:681-687.
66. Gregory CA, Singh H, Perry AS, et al. The Wnt signaling inhibitor dickkopf-1 is required for reentry into the cell cycle of human adult stem cells from bone marrow. J Biol Chem. 2003;278:28067-28078.
67. Gilbert L, He X, Farmer P, et al. Expression of the osteoblast differentiation factor RUNX2 (Cbfa1/AML3/Pebp2alpha A) is inhibited by tumor necrosis factor-alpha. J Biol Chem. 2002;277:2695-2701.
68. Satija NK, Gurudutta GU, Sharma S, et al. Mesenchymal stem cells: molecular targets for tissue engineering. Stem Cells Dev. 2007;16:7-23.
69. Molofsky AV, Pardal R, Morrison SJ. Diverse mechanisms regulate stem cell self-renewal. Curr Opin Cell Biol. 2004;16:700-707.
70. Izadpanah R, Trygg C, Patel B, et al. Biologic properties of mesenchymal stem cells derived from bone marrow and adipose tissue. J Cell Biochem. 2006;99:1285-1297.
71. Sitcheran R, Cogswell PC, Baldwin AS, Jr. NF-kappaB mediates inhibition of mesenchymal cell differentiation through a posttranscriptional gene silencing mechanism. Genes Dev. 2003;17:2368-2373.
72. Song L, Tuan RS. Transdifferentiation potential of human mesenchymal stem cells derived from bone marrow. Faseb J. 2004;18:980-982.
73. Ferrari G, Cusella-De Angelis G, Coletta M, et al. Muscle regeneration by bone marrow-derived myogenic progenitors. Science. 1998;279:1528-1530.
74. Hess D, Li L, Martin M, et al. Bone marrow-derived stem cells initiate pancreatic regeneration. Nat Biotechnol. 2003;21:763-770.
75. Komori T. Regulation of osteoblast differentiation by transcription factors. J Cell Biochem. 2006;99:1233-1239.
76. Nakashima K, Zhou X, Kunkel G, et al. The novel zinc finger-containing transcription factor osterix is required for osteoblast differentiation and bone formation. Cell. 2002;108:17-29.
77. Friedman MS, Long MW, Hankenson KD. Osteogenic differentiation of human mesenchymal stem cells is regulated by bone morphogenetic protein-6. J Cell Biochem. 2006;98:538-554.
78. Tu X, Joeng KS, Nakayama KI, et al. Noncanonical Wnt signaling through G protein-linked PKCdelta activation promotes bone formation. Dev Cell. 2007;12:113-127.
79. Schmitt B, Ringe J, Haupl T, et al. BMP2 initiates chondrogenic lineage development of adult human mesenchymal stem cells in high-density culture. Differentiation. 2003;71:567-577.
80. Hatakeyama Y, Tuan RS, Shum L. Distinct functions of BMP4 and GDF5 in the regulation of chondrogenesis. J Cell Biochem. 2004;91:1204-1217.
81. Hwang SG, Yu SS, Lee SW, et al. Wnt-3a regulates chondrocyte differentiation via c-Jun/AP-1 pathway. FEBS Lett. 2005;579:4837-4842.

82. Hartmann C. A Wnt canon orchestrating osteoblastogenesis. Trends Cell Biol. 2006;16:151-158.
83. Kahata K, Hayashi M, Asaka M, et al. Regulation of transforming growth factor-beta and bone morphogenetic protein signalling by transcriptional coactivator GCN5. Genes Cells. 2004;9:143-151.
84. Reinhold MI, Kapadia RM, Liao Z, et al. The Wnt-inducible transcription factor Twist1 inhibits chondrogenesis. J Biol Chem. 2006;281:1381-1388.
85. Tuli R, Tuli S, Nandi S, et al. Transforming growth factor-beta-mediated chondrogenesis of human mesenchymal progenitor cells involves N-cadherin and mitogen-activated protein kinase and Wnt signaling cross-talk. J Biol Chem. 2003;278:41227-41236.
86. Rosen ED, MacDougald OA. Adipocyte differentiation from the inside out. Nat Rev Mol Cell Biol. 2006;7:885-896.
87. Lecka-Czernik B, Moerman EJ, Grant DF, et al. Divergent effects of selective peroxisome proliferator-activated receptor-gamma 2 ligands on adipocyte versus osteoblast differentiation. Endocrinology. 2002;143:2376-2384.
88. Nuttall ME, Gimble JM. Controlling the balance between osteoblastogenesis and adipogenesis and the consequent therapeutic implications. Curr Opin Pharmacol. 2004;4:290-294.
89. Linhart HG, Ishimura-Oka K, DeMayo F, et al. C/EBPalpha is required for differentiation of white, but not brown, adipose tissue. Proc Natl Acad Sci U S A. 2001;98:12532-12537.
90. Ross SE, Hemati N, Longo KA, et al. Inhibition of adipogenesis by Wnt signaling. Science. 2000;289:950-953.
91. McBeath R, Pirone DM, Nelson CM, et al. Cell shape, cytoskeletal tension, and RhoA regulate stem cell lineage commitment. Dev Cell. 2004;6:483-495.
92. Minguell JJ, Erices A, Conget P. Mesenchymal stem cells. Exp Biol Med (Maywood). 2001;226:507-520.
93. Tang YL, Zhao Q, Zhang YC, et al. Autologous mesenchymal stem cell transplantation induce VEGF and neovascularization in ischemic myocardium. Regul Pept. 2004;117:3-10.
94. Pak HN, Qayyum M, Kim DT, et al. Mesenchymal stem cell injection induces cardiac nerve sprouting and increased tenascin expression in a Swine model of myocardial infarction. J Cardiovasc Electrophysiol. 2003;14:841-848.
95. Caplan AI, Dennis JE. Mesenchymal stem cells as trophic mediators. J Cell Biochem. 2006;98:1076-1084.
96. Pawelec G, Rehbein A, Schlotz E, et al. Cytokine modulation of TH1/TH2 phenotype differentiation in directly alloresponsive CD4+ human T cells. Transplantation. 1996;62:1095-1101.
97. Wood KJ, Sakaguchi S. Regulatory T cells in transplantation tolerance. Nat Rev Immunol. 2003;3:199-210.
98. Koc ON, Day J, Nieder M, et al. Allogeneic mesenchymal stem cell infusion for treatment of metachromatic leukodystrophy (MLD) and Hurler syndrome (MPS-IH). Bone Marrow Transplant. 2002;30:215-222.
99. Koc ON, Gerson SL, Cooper BW, et al. Rapid hematopoietic recovery after coinfusion of autologous-blood stem cells and culture-expanded marrow mesenchymal stem cells in advanced breast cancer patients receiving high-dose chemotherapy. J Clin Oncol. 2000;18:307-316.

100. Deng W, Han Q, Liao L, et al. Allogeneic bone marrow-derived flk-1+Sca-1- mesenchymal stem cells leads to stable mixed chimerism and donor-specific tolerance. Exp Hematol. 2004;32:861-867.
101. Bartholomew A, Sturgeon C, Siatskas M, et al. Mesenchymal stem cells suppress lymphocyte proliferation in vitro and prolong skin graft survival in vivo. Exp Hematol. 2002;30:42-48.
102. Schwarz EJ, Alexander GM, Prockop DJ, et al. Multipotential marrow stromal cells transduced to produce L-DOPA: engraftment in a rat model of Parkinson disease. Hum Gene Ther. 1999;10:2539-2549.
103. Toma C, Pittenger MF, Cahill KS, et al. Human mesenchymal stem cells differentiate to a cardiomyocyte phenotype in the adult murine heart. Circulation. 2002;105:93-98.
104. Quesenberry PJ, Colvin G, Abedi M. Perspective: fundamental and clinical concepts on stem cell homing and engraftment: a journey to niches and beyond. Exp Hematol. 2005;33:9-19.
105. Lapidot T, Dar A, Kollet O. How do stem cells find their way home? Blood. 2005;106:1901-1910.
106. Zhu H, Mitsuhashi N, Klein A, et al. The role of the hyaluronan receptor CD44 in mesenchymal stem cell migration in the extracellular matrix. Stem Cells. 2006;24:928-935.
107. Kolf CM, Cho E, Tuan RS. Mesenchymal stromal cells. Biology of adult mesenchymal stem cells: regulation of niche, self-renewal and differentiation. Arthritis Res Ther. 2007;9:204.
108. Fink T, Abildtrup L, Fogd K, et al. Induction of adipocyte-like phenotype in human mesenchymal stem cells by hypoxia. Stem Cells. 2004;22:1346-1355.
109. Grayson WL, Zhao F, Izadpanah R, et al. Effects of hypoxia on human mesenchymal stem cell expansion and plasticity in 3D constructs. J Cell Physiol. 2006;207:331-339.
110. Martin-Rendon E, Hale SJ, Ryan D, et al. Transcriptional Profiling of Human Cord Blood CD133+ and Cultured Bone Marrow Mesenchymal Stem Cells in Response to Hypoxia. Stem Cells. 2007;25:1003-1012.
111. Mostafa SS, Miller WM, Papoutsakis ET. Oxygen tension influences the differentiation, maturation and apoptosis of human megakaryocytes. Br J Haematol. 2000;111:879-889.
112. Lennon DP, Edmison JM, Caplan AI. Cultivation of rat marrow-derived mesenchymal stem cells in reduced oxygen tension: effects on in vitro and in vivo osteochondrogenesis. J Cell Physiol. 2001;187:345-355.
113. Chow DC, Wenning LA, Miller WM, et al. Modeling pO(2) distributions in the bone marrow hematopoietic compartment. I. Krogh's model. Biophys J. 2001;81:675-684.
114. Opara EC. Oxidative stress. Dis Mon. 2006;52:183-198.
115. Voeikov VL. Reactive oxygen species--(ROS) pathogens or sources of vital energy? Part 1. ROS in normal and pathologic physiology of living systems. J Altern Complement Med. 2006;12:111-118.
116. Verfaillie C. lecture, Oslo, February 2006.
117. Boyum A. Separation of leukocytes from blood and bone marrow. Introduction. Scand J Clin Lab Invest Suppl. 1968;97:7.
118. Arya M, Shergill IS, Williamson M, et al. Basic principles of real-time quantitative PCR. Expert Rev Mol Diagn. 2005;5:209-219.
119. Kubista M, Andrade JM, Bengtsson M, et al. The real-time polymerase chain reaction. Mol Aspects Med. 2006;27:95-125.
120. Livak KJ, Schmittgen TD. Analysis of relative gene expression data using real-time quantitative PCR and the 2(-Delta Delta C(T)) Method. Methods. 2001;25:402-408.

121. Valasek MA, Repa JJ. The power of real-time PCR. Adv Physiol Educ. 2005;29:151-159.
122. Schmittgen TD, Zakrajsek BA. Effect of experimental treatment on housekeeping gene expression: validation by real-time, quantitative RT-PCR. J Biochem Biophys Methods. 2000;46:69-81.
123. Mount DW. Bioinformatics: Sequence and genome analysis: Cold spring harbor laboratory press; 2004: 612-659.
124. Hardiman G. Microarray platforms--comparisons and contrasts. Pharmacogenomics. 2004;5:487-502.
125. Holloway AJ, van Laar RK, Tothill RW, et al. Options available--from start to finish--for obtaining data from DNA microarrays II. Nat Genet. 2002;32 Suppl:481-489.
126. Gunderson KL, Kruglyak S, Graige MS, et al. Decoding randomly ordered DNA arrays. Genome Res. 2004;14:870-877.
127. Doerr HW, Cinatl J, Sturmer M, et al. Prions and orthopedic surgery. Infection. 2003;31:163-171.
128. Selvaggi TA, Walker RE, Fleisher TA. Development of antibodies to fetal calf serum with arthus-like reactions in human immunodeficiency virus-infected patients given syngeneic lymphocyte infusions. Blood. 1997;89:776-779.
129. Stenderup K, Justesen J, Clausen C, et al. Aging is associated with decreased maximal life span and accelerated senescence of bone marrow stromal cells. Bone. 2003;33:919-926.
130. Shay JW, Wright WE. Senescence and immortalization: role of telomeres and telomerase. Carcinogenesis. 2005;26:867-874.
131. Simonsen JL, Rosada C, Serakinci N, et al. Telomerase expression extends the proliferative life-span and maintains the osteogenic potential of human bone marrow stromal cells. Nat Biotechnol. 2002;20:592-596.
132. Chambers I, Smith A. Self-renewal of teratocarcinoma and embryonic stem cells. Oncogene. 2004;23:7150-7160.
133. Bubner B, Gase K, Baldwin IT. Two-fold differences are the detection limit for determining transgene copy numbers in plants by real-time PCR. BMC Biotechnol. 2004;4:14.
134. Ducy P, Karsenty G. The family of bone morphogenetic proteins. Kidney Int. 2000;57:2207-2214.
135. Boskey AL, Paschalis EP, Binderman I, et al. BMP-6 accelerates both chondrogenesis and mineral maturation in differentiating chick limb-bud mesenchymal cell cultures. J Cell Biochem. 2002;84:509-519.
136. Ohnishi S, Yasuda T, Kitamura S, et al. Effect of hypoxia on gene expression of bone marrow-derived mesenchymal stem cells and mononuclear cells. Stem Cells. 2007;25:1166-1177.
137. Stichtenoth DO, Thoren S, Bian H, et al. Microsomal prostaglandin E synthase is regulated by proinflammatory cytokines and glucocorticoids in primary rheumatoid synovial cells. J Immunol. 2001;167:469-474.
138. Minchenko O, Opentanova I, Minchenko D, et al. Hypoxia induces transcription of 6-phosphofructo-2-kinase/fructose-2,6-biphosphatase-4 gene via hypoxia-inducible factor-1alpha activation. FEBS Lett. 2004;576:14-20.
139. Minchenko OH, Opentanova IL, Ogura T, et al. Expression and hypoxia-responsiveness of 6-phosphofructo-2-kinase/fructose-2,6-bisphosphatase 4 in mammary gland malignant cell lines. Acta Biochim Pol. 2005;52:881-888.

140. Le Jan S, Le Meur N, Cazes A, et al. Characterization of the expression of the hypoxia-induced genes neuritin, TXNIP and IGFBP3 in cancer. FEBS Lett. 2006;580:3395-3400.
141. Morey JS, Ryan JC, Van Dolah FM. Microarray validation: factors influencing correlation between oligonucleotide microarrays and real-time PCR. Biol Proced Online. 2006;8:175-193.
142. Grayson WL, Zhao F, Bunnell B, et al. Hypoxia enhances proliferation and tissue formation of human mesenchymal stem cells. Biochem Biophys Res Commun. 2007.
143. Malladi P, Xu Y, Chiou M, et al. Effect of reduced oxygen tension on chondrogenesis and osteogenesis in adipose-derived mesenchymal cells. Am J Physiol Cell Physiol. 2006;290:C1139-1146.
144. Wang DW, Fermor B, Gimble JM, et al. Influence of oxygen on the proliferation and metabolism of adipose derived adult stem cells. J Cell Physiol. 2005;204:184-191.
145. Chan DA, Sutphin PD, Yen SE, et al. Coordinate regulation of the oxygen-dependent degradation domains of hypoxia-inducible factor 1 alpha. Mol Cell Biol. 2005;25:6415-6426.
146. Carmeliet P, Dor Y, Herbert JM, et al. Role of HIF-1alpha in hypoxia-mediated apoptosis, cell proliferation and tumour angiogenesis. Nature. 1998;394:485-490.
147. Jiang BH, Semenza GL, Bauer C, et al. Hypoxia-inducible factor 1 levels vary exponentially over a physiologically relevant range of O2 tension. Am J Physiol. 1996;271:C1172-1180.
148. Rolfs A, Kvietikova I, Gassmann M, et al. Oxygen-regulated transferrin expression is mediated by hypoxia-inducible factor-1. J Biol Chem. 1997;272:20055-20062.
149. Gerber HP, Condorelli F, Park J, et al. Differential transcriptional regulation of the two vascular endothelial growth factor receptor genes. Flt-1, but not Flk-1/KDR, is up-regulated by hypoxia. J Biol Chem. 1997;272:23659-23667.
150. Covello KL, Kehler J, Yu H, et al. HIF-2alpha regulates Oct-4: effects of hypoxia on stem cell function, embryonic development, and tumor growth. Genes Dev. 2006;20:557-570.
151. Yun Z, Maecker HL, Johnson RS, et al. Inhibition of PPAR gamma 2 gene expression by the HIF-1-regulated gene DEC1/Stra13: a mechanism for regulation of adipogenesis by hypoxia. Dev Cell. 2002;2:331-341.
152. Campbell. Biology: Benjamin Cummings; 2002: 363-368.